

OBSERVER DEPENDENCE IN HOLOGRAPHIC ENTANGLEMENT ENTROPY

by

Zachary A Polonsky

© Copyright by Zachary A Polonsky, 2018

All Rights Reserved

A thesis submitted to the Faculty and the Board of Trustees of the Colorado School of Mines in partial fulfillment of the requirements for the degree of Master of Science (Applied Physics).

Golden, Colorado

Date _____

Signed: _____
Zachary A Polonsky

Signed: _____
Dr. Jeff Squier
Thesis Advisor

Signed: _____
Dr. Alex Flourney
Thesis Advisor

Golden, Colorado

Date _____

Signed: _____
Dr. Uwe Greife
Professor and Head
Department of Physics

ABSTRACT

The Anti-de Sitter/Conformal Field Theory (AdS/CFT) correspondence conjectures a duality between gravitational theories in asymptotically Anti-de Sitter (AdS) spacetimes and non-gravitational quantum conformal field theories (CFTs) defined on the boundary of the gravitational spacetimes. This correspondence provides strong evidence for the holographic nature of gravity while also giving insight into the relationship between gravity and quantum mechanics. These ideas have been sharpened by the holographic entanglement entropy results of Ryu, Takayanagi, Rangamani, and Hubeny. However, most holographic entanglement entropy results are restricted to the technically simple setting of $(2+1)$ -dimensional gravity. These have suggested a distinct relationship between thermal entropy of black holes in the gravitational theory and entanglement entropy corresponding to thermal states in the CFT. In higher dimensions, there exist black holes whose event horizon area (and seemingly thermal properties) are highly observer dependent. We find that, although this observer dependence does not carry over to the holographic entanglement entropy, there is an indication of a coordinate system which is best adapted for the holographic calculation. These coordinates only cover two regions of the spacetime which exactly correspond to the regions of the CFT on which particle modes are well defined and so we see that the holographic calculation in the spacetime is capable of predicting parts of the CFT where particles cannot exist.

TABLE OF CONTENTS

ABSTRACT	iii
LIST OF FIGURES	vi
LIST OF SYMBOLS	ix
LIST OF ABBREVIATIONS	x
ACKNOWLEDGMENTS	xi
DEDICATION	xii
CHAPTER 1 INTRODUCTION	1
CHAPTER 2 BACKGROUND	7
2.1 General Relativity	7
2.2 Killing Vectors	9
2.3 Conformal Killing Vectors	11
2.4 Embedding Spaces	11
2.5 Anti-de Sitter Spacetime	14
2.6 Quotients	18
2.7 Topological Black Holes: The BTZ Black Hole	19
2.8 (3+1)-Dimensional Topological Black Hole	26
CHAPTER 3 HOLOGRAPHIC ENTANGLEMENT ENTROPY	31
3.1 Classical Entropy	31
3.2 Entanglement Entropy	32
3.3 Entanglement Entropy in QFTs	33

3.4	Spacetime Entropy	35
3.4.1	Area-Law	36
3.4.2	Semiclassical Thermodynamic Calculations	39
3.5	Holographic Entanglement Entropy	44
3.5.1	(1+1)-Dimensional CFT at Zero Temperature	45
3.5.2	(1+1)-Dimensional CFT at Finite Temperature	48
3.5.3	BTZ Boundary Theory	52
3.5.4	Strip on Boundary of AdS_d	54
CHAPTER 4 TIME-DEPENDENT BLACK HOLES IN HOLOGRAPHIC ENTANGLEMENT ENTROPY		57
4.1	Observer-Dependent Event Horizon	57
4.2	Holographic Calculation	58
4.3	Thermodynamics of the Topological Black Hole	61
4.4	Restriction of Particle Modes on Boundary	62
CHAPTER 5 CONCLUSIONS AND OUTLOOK		66
REFERENCES CITED		68

LIST OF FIGURES

Figure 1.1	Examples of duality in AdS/CFT. Global AdS is dual to a vacuum state, a gravitational wave is dual to a particle-like excitation, and an eternal black hole is dual to a thermal state.	2
Figure 1.2	Lightlike trajectories in Minkowski space as viewed by inertial observers are given as lines at 45-degrees in the $x - t$ plane. In this example, the light pulse was emitted at $x = 0, t = 0$	3
Figure 1.3	Lightlike trajectories in Minkowski space as viewed by accelerated observers are warped from those seen by inertial observers. The black line corresponds to $a = 0.1$, the blue line corresponds to $a = 0.5$, and the red line corresponds to $a = 1$	4
Figure 1.4	An accelerated observer at constant ξ emits a light pulse at time $t_i < 0$. The light crosses the surface $t = x$ at time $t_c \geq 0$. Since light travels on null trajectories, the light propagates parallel to either the $t = x$ or $t = -x$ surfaces and therefore cannot cross the $t = x$ surface again. Therefore, the constant ξ observer sees an acceleration horizon at $t = x$. A similar argument for past-directed light pulses can be made for the $t = -x$ surface.	6
Figure 2.1	The 2-sphere can either be parameterized by two coordinates, θ and ϕ , on the surface itself, or as a submanifold of \mathbb{R}^3 described by the constraint equation $x^2 + y^2 + z^2 = 1$	12
Figure 2.2	Cross section of AdS_d at $T_2 = X_{n+2} = 0$ described by surface (2.21) embedded in $\mathbb{R}^{2,d-1}$	14
Figure 2.3	Example of how causality is violated with closed timelike curves. If the time coordinate, t , is periodic, we can have trajectories of massive particles (dashed line) which loop back on themselves in time. However, if two causally connected events, A and B, occur on this trajectory, it is impossible to say which caused the other, violating causality.	15
Figure 2.4	Lightlike trajectories for AdS_d in spherical coordinates. These begin at $t = 0$ like those in Minkowski space, but then flatten out as $t \rightarrow \pi/2$	16

Figure 2.5	Penrose diagram of global AdS with angular coordinates suppressed. The time coordinate runs in the vertical direction and the radial coordinate runs in the horizontal direction. The line on the left represents the origin of the space ($r = 0$) and the line on the right represents infinity ($r = \infty$). The dashed line shows the trajectory of a lightlike particle which reaches infinity and returns to $r = 0$ in finite time.	17
Figure 2.6	The act of quotienting \mathbb{R}^2 to obtain the cylinder. First, we identify that \mathbb{R}^2 has Killing vector associated with translations in x . Then, we cut the space orthogonal to the flow of this Killing vector. Finally, we identify the two cuts to change the topology of the space. Dashed lines extend to infinity in this figure.	19
Figure 2.7	Special surfaces induced by a quotient generated by ξ in the $T_2 - X_2$ plane. The hyperbola given by $X_2^2 - T_2^2 = -1$ is the singularity, while the lines $X_2^2 - T_2^2 = 0$ are the event horizons. A and B are spacetime points at which light pulses are emitted in the exterior and interior of the black hole, respectively. The corresponding future-directed and past-directed light cones are 45-degree lines.	21
Figure 2.8	Maximally extended BTZ spacetime. Regions I and IV are asymptotically distinct exterior regions, region II is the black hole interior and region III is the white hole interior. This space is geodesically complete since any null geodesic either terminates at a singularity or extends to infinity.	26
Figure 2.9	Special surfaces induced by a quotient generated by ξ in the $T_2 - X_2 - X_3$ hyperplane. The hyperboloid given by $X_2^2 + X_3^2 - T_2^2 = -1$ is the singularity (red), while the cones $X_2^2 + X_3^2 - T_2^2 = 0$ are the event horizons (black).	27
Figure 3.1	QFT on subregion A is entangled with the rest of QFT on \bar{A} and therefore the entanglement entropy for region A is nonzero. Since the total QFT is pure, the entanglement entropy of QFT on $A \cup \bar{A}$ is zero.	34
Figure 3.2	To calculate the entanglement entropy of the CFT on region A with the CFT on region \bar{A} , we calculate the area of the extremal-area surface, γ , which ends on the boundary of A , ∂A	45
Figure 3.3	The entanglement entropy of the CFT on region A with length $2R$ can be calculated by the minimal area surface, γ , given by semicircles of radius R which intersect the boundary at right angles.	47

Figure 3.4	The minimal surface γ will have a critical point at $r = r_*$. Since γ is uniquely specified by either r_* or the length of the region A of the boundary, $2R$, we can use either to give γ	49
Figure 3.5	Minimal area surface, γ (red), corresponding to different sizes of region A (green) on the boundary. When A reaches a certain size, $\gamma' \cup H < \gamma$ becomes the minimal area surface, and when A is the full boundary, only the area of the event horizon remains.	52
Figure 3.6	Penrose diagram of the maximally extended BTZ black hole. Here, there are two distinct boundaries, D_R and D_L , on which η_b is a timelike Killing vector. On D_R , the t -component of η_b ($\eta_b^{(t)}$) is positive, and so we associate this region with positive energy modes, while on D_L , $\eta_b^{(t)}$ is negative, so we associate this region with negative energy modes.	54
Figure 3.7	Minimal area surface, γ (green) corresponding to strip A of the boundary (red). The strip has length L and width R	55
Figure 4.1	Diagram of the boundary of the topological black hole. The dashed circle represents $t = \tau = 0$, where η_b is timelike over the whole boundary. We see two distinct regions on the boundary where η_b is timelike, one where the time component, $\eta_b^{(t)}$, is positive, which we associate with positive energy modes (red), while on the other, $\eta_b^{(t)}$ is negative, which we associate with negative energy modes (blue). This figure is in contrast to Figure 3.6 since the latter shows two distinct boundaries where the modes are defined, while this shows two regions of the same boundary where modes are defined.	65

LIST OF SYMBOLS

Differential line element of space(time) (metric)	ds
Ricci Tensor	$R_{\mu\nu}$
Ricci Scalar	R
Cosmological Constant	Λ
Metric tensor	$g_{\mu\nu}$
Christoffel symbol	$\Gamma_{\mu\nu}^{\lambda}$
Covariant derivative	∇_{μ}
Killing vector	K^{μ}
Killing vector (coordinate-invariant form)	ξ or η
Conformal factor	Ω^2
Unphysical differential line element (unphysical metric)	$d\tilde{s}$
Trace	Tr
Determinate of metric	g
Differential line element on submanifold (induced metric)	$d\sigma$
Induced metric	$h_{\mu\nu}$
Determinate of induced metric	h

LIST OF ABBREVIATIONS

Anti-de Sitter AdS
Conformal Field Theory CFT
Quantum Field Theory QFT
Bañados-Tietelboim-Zanelli BTZ
Holographic Entanglement Entropy HEE

ACKNOWLEDGMENTS

First and foremost, I would like to acknowledge Dr. Alex Flournoy, who took the time out of his already busy life to be my advisor for this project. I have learned more about theoretical physics under Alex than I ever could have hoped. I would also like to acknowledge my thesis committee, Dr. Jeff Squier, Dr. Kyle Leach, and Dr. Laith Haddad for allowing me to pursue this project, despite it being outside many of their research interests. Thank you all very much.

This thesis is dedicated to my family, friends, and all others who have supported me throughout the meandering journey of my life.

CHAPTER 1

INTRODUCTION

The Anti-de Sitter/Conformal Field Theory (AdS/CFT) correspondence, originally proposed by Maldacena in 1997, realizes an equivalence between gravitational theories in a d -dimensional asymptotically AdS spacetime (also known as the “bulk”) and non-gravitational CFTs defined on a fixed $(d - 1)$ -dimensional spacetime which shares the same geometry as the boundary of the asymptotically AdS spacetime [2].

Quantum field theories (QFTs) in flat spacetime typically exhibit Lorentz invariance and invariance under spacetime translations. CFTs are QFTs that remain invariant under the larger group of conformal transformations which include not only Lorentz transformations and spacetime translations but also scale transformations and special conformal transformations [4].

That there is a duality between these two different theories implies that the physics in one theory is equally described by the physics in the other theory. This is particularly surprising since one side utilizes a field theory on a fixed geometry, while the other side uses a dynamical geometry in one spacetime dimension higher. As examples, global AdS is dual to the vacuum state of the CFT, a gravitational wave in the bulk is dual to a particle-like excitation in the CFT, and an eternal black hole in the bulk is dual to a thermal state in the CFT (Figure 1.1) [2, 5, 17].

Though the AdS/CFT duality is conjectured to hold for all physical phenomena in both the geometric bulk and the quantum boundary theory, there is a certain type of entropy which is unique to quantum systems. The geometric dual to this particular type of entropy was originally proposed by Ryu-Takayanagi in 2006, and generalized to a covariant formalism by Hubeny-Rangamani-Takayanagi in 2007 [10, 11]. However, in general relativity, it is a common occurrence that different observers experience the same universe in different ways.

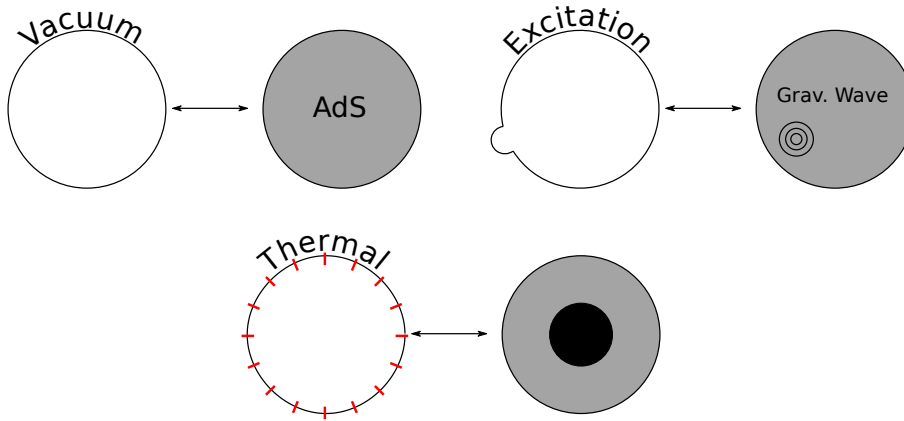


Figure 1.1: Examples of duality in AdS/CFT. Global AdS is dual to a vacuum state, a gravitational wave is dual to a particle-like excitation, and an eternal black hole is dual to a thermal state.

For example, an observer outside of a static black hole does not have access to the entire spacetime since they cannot see past the event horizon, but an observer falling into the black hole will eventually be able to see the entire spacetime, including the black hole interior.

As a more concrete example, consider Minkowski space (in $(1 + 1)$ dimensions for simplicity) with differential line element

$$ds^2 = -dt^2 + dx^2 \quad (1.1)$$

where we have used natural units where $c = 1$. If we want to examine the paths which light takes (i.e. null geodesics), we can set $ds^2 = 0$

$$dt^2 = dx^2 \Rightarrow \frac{dt}{dx} = \pm 1 \Rightarrow t(x) = \pm x \mp x_0 \quad (1.2)$$

where x_0 is where the light is emitted at $t = 0$. This gives us the usual light cones of special relativity shown in Figure 1.2.

If we wish to find these same trajectories for a non-inertial observer moving at some acceleration $\alpha = \text{const.}$, we can first define a 4-acceleration

$$a^\mu = \frac{d^2 x^\mu}{d\tau^2} \quad (1.3)$$

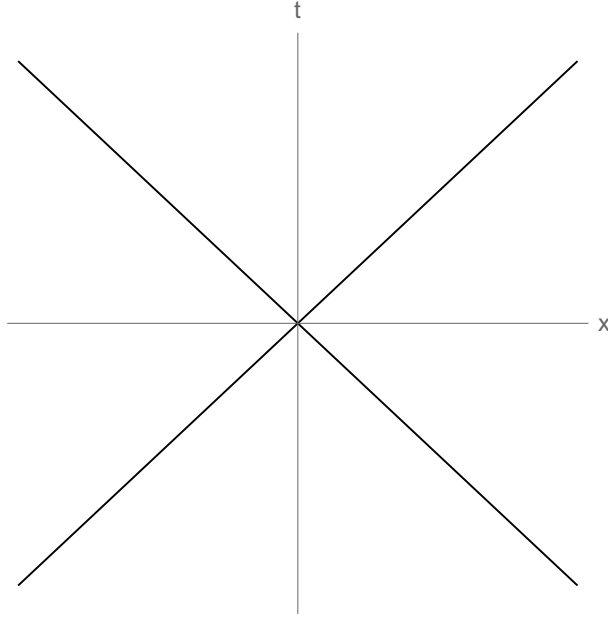


Figure 1.2: Lightlike trajectories in Minkowski space as viewed by inertial observers are given as lines at 45-degrees in the $x - t$ plane. In this example, the light pulse was emitted at $x = 0, t = 0$.

where τ is the proper time, or the time measured by a clock in a co-moving frame. Since the magnitude of the 4-acceleration is just α , we have

$$\sqrt{a^\mu a_\mu} = \sqrt{-\left(\frac{d^2 t}{d\tau^2}\right)^2 + \left(\frac{d^2 x}{d\tau^2}\right)^2} = \alpha \quad (1.4)$$

which has the solution

$$\begin{aligned} t(\tau) &= \frac{1}{\alpha} \sinh(\alpha\tau) \\ x(\tau) &= \frac{1}{\alpha} \cosh(\alpha\tau). \end{aligned} \quad (1.5)$$

Using this result, we can now intuit new coordinates

$$\begin{aligned} t &= \left(\frac{1}{a} + \xi\right) \sinh(a\eta) \\ x &= \left(\frac{1}{a} + \xi\right) \cosh(a\eta) \end{aligned} \quad (1.6)$$

where a is some positive constant, $\eta \in (-\infty, \infty)$, and $\xi \in [-1/a, \infty)$. The metric (1.1) becomes

$$ds^2 = -(1 + a\xi)^2 d\eta^2 + d\xi^2. \quad (1.7)$$

If we take $\eta = \tau$ to be proper time, the magnitude of the 4-acceleration becomes

$$\sqrt{a^\mu a_\mu} = a(1 + a\xi). \quad (1.8)$$

Generally, a coordinate system is adapted to observers at fixed spatial points, so fixed x in coordinates corresponding to metric (1.1) and fixed ξ in coordinates corresponding to metric (1.7) [18]. From the form of (1.4) and (1.8), we can see that observers of constant ξ are uniformly accelerating.

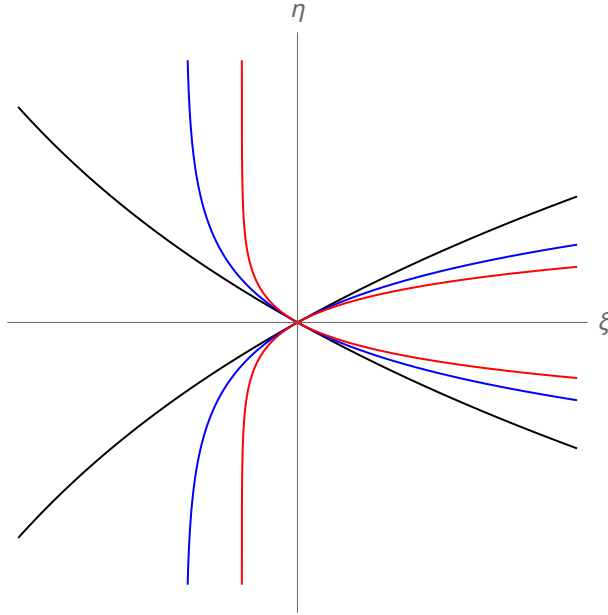


Figure 1.3: Lightlike trajectories in Minkowski space as viewed by accelerated observers are warped from those seen by inertial observers. The black line corresponds to $a = 0.1$, the blue line corresponds to $a = 0.5$, and the red line corresponds to $a = 1$.

Now we can ask, what does an accelerated observer in flat space see? The first thing we notice is that a uniformly accelerated observer does not see light take the same trajectories

as an inertial observer. Setting $ds^2 = 0$ in (1.7), we find

$$(1 + a\xi)^2 d\eta^2 = d\xi^2 \Rightarrow \eta(\xi) = \pm \int \frac{d\xi}{1 + a\xi} = \pm \frac{1}{a} \log \left(\frac{1 + a\xi}{1 + a\xi_0} \right) \quad (1.9)$$

where ξ_0 is where the light is emitted at $\eta = 0$. These trajectories are shown in Figure 1.3. In the limit where we have $a \rightarrow 0$, $\eta(\xi) = \pm(\xi - \xi_0)$, which is the trajectory an unaccelerated observer would see. This is exactly what we would expect since, when $a = 0$, the metric (1.7) reduces to the metric in inertial coordinates (1.1).

More relevant to this thesis than the new perceived paths of light is the introduction of acceleration horizons. From the coordinate ranges of ξ and η , we can see that these coordinates only cover the region of Minkowski space where $t \in (-\infty, \infty)$ and $x > 0$. Furthermore, an observer of constant ξ travels along the hyperbola given by

$$x^2 - t^2 = \frac{1}{a} + \xi, \quad (1.10)$$

bounded by the surfaces $t = \pm x$. However, these surfaces are just null (light-like) trajectories for an unaccelerated observer. Consider an accelerated observer of constant ξ emitting a light pulse at inertial time $t = t_i < 0$. At some point $t = t_c \geq 0$, the accelerated observer sees the light pulse cross the null surface, but for any time $t > t_c$, it is impossible for this light pulse to return to the accelerated observer. Therefore, the accelerated observer cannot receive signals from beyond the surface, analogous to a black hole event horizon (Figure 1.4).

From the example of an accelerated observer in Minkowski space, it is clear that, in general relativity different observers can experience the same spacetime in different ways. This thesis will mainly focus on how these observer-dependences translate to a dual Conformal Field Theory description in the conjectured AdS/CFT correspondence.

In chapter 2, we present the background material necessary for this thesis. In chapter 3, we discuss different types of entropy in both quantum and gravitational systems, give methods of calculation in the two different systems separately, and finally present the holographic entanglement entropy conjecture. In chapter 4, we give the results of our work, and in chapter 5, we give a brief summary of the results and outlook for future work.

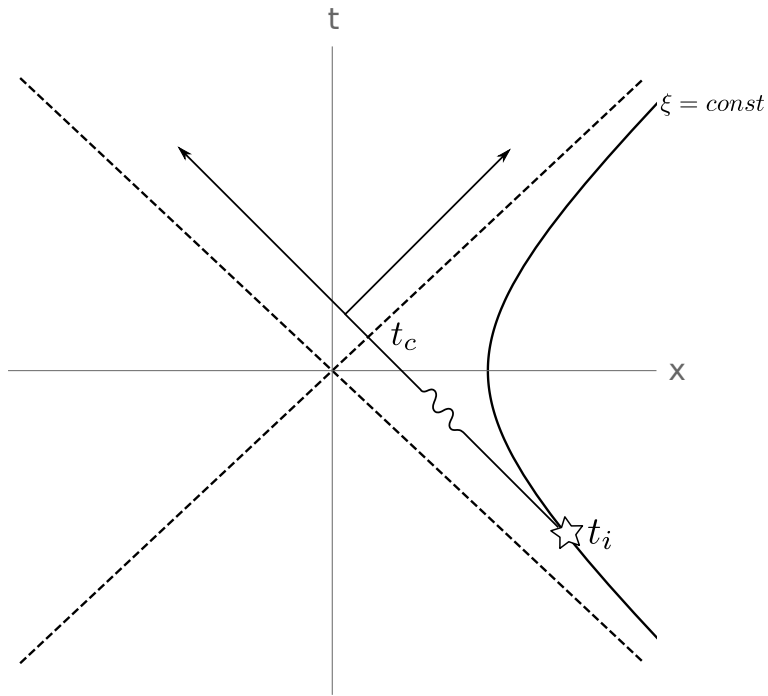


Figure 1.4: An accelerated observer at constant ξ emits a light pulse at time $t_i < 0$. The light crosses the surface $t = x$ at time $t_c \geq 0$. Since light travels on null trajectories, the light propagates parallel to either the $t = x$ or $t = -x$ surfaces and therefore cannot cross the $t = x$ surface again. Therefore, the constant ξ observer sees an acceleration horizon at $t = x$. A similar argument for past-directed light pulses can be made for the $t = -x$ surface.

CHAPTER 2

BACKGROUND

We will be mostly working from the geometric side of the AdS/CFT correspondence, and so it is important to first become comfortable with the language of general relativity as well as the tools used to construct and analyze the spacetime of interest: the $(3 + 1)$ -dimensional topological black hole. Section 2.1 introduces the field equation of general relativity, gives physical intuition into the meaning of the equation, and justifies the use of coordinate transformations as a gauge freedom. Section 2.2 introduces a method of identifying symmetries of a space through the use of Killing's equation, which will be vital for building quotient spaces and for finding regions on the boundary theory which support particles. Section 2.3 extends the results of section 2.2 to conformal Killing vectors which preserve the metric of a space up to a scaling factor. Section 2.4 provides an easier way of analyzing complicated spaces by embedding the space in a higher dimensional one to simplify calculations. We discuss the benefits as well as the disadvantages of using embedding spaces. Using the concepts of section 2.4, we define Anti-de Sitter spacetime and give some of its properties in section 2.5. In section 2.6, we show a way of constructing globally non-trivial spaces from globally trivial ones while keeping the simple local properties of the original spaces. Finally, we introduce the $(2 + 1)$ - and $(3 + 1)$ -dimensional topological black holes in sections 2.7 and 2.8 using the ideas introduced in previous sections.

2.1 General Relativity

We begin the discussion of general relativity with Einstein's field equation

$$R_{\mu\nu} - \frac{1}{2}Rg_{\mu\nu} + \Lambda g_{\mu\nu} = 8\pi G_N T_{\mu\nu}. \quad (2.1)$$

where $g_{\mu\nu}$ is the μ, ν component of the metric tensor, Λ is the cosmological constant, G_N is Newton's gravitational constant, and $T_{\mu\nu}$ is the μ, ν component of the energy-momentum

tensor [15, 18]. We will only focus on vacuum solutions, where $T_{\mu\nu} = 0$. $R_{\mu\nu}$ is the μ, ν component of the Ricci tensor, given by

$$\begin{aligned} R_{\mu\nu} &= \partial_\lambda \Gamma_{\mu\nu}^\lambda - \partial_\nu \Gamma_{\mu\lambda}^\lambda + \Gamma_{\mu\nu}^\phi \Gamma_{\phi\lambda}^\lambda - \Gamma_{\mu\lambda}^\phi \Gamma_{\phi\nu}^\lambda, \\ \Gamma_{\mu\nu}^\lambda &= \frac{1}{2} g^{\lambda\phi} (\partial_\mu g_{\phi\nu} + \partial_\nu g_{\phi\mu} - \partial_\phi g_{\mu\nu}) \end{aligned} \quad (2.2)$$

where $\Gamma_{\mu\nu}^\lambda$ are the components of the Christoffel symbols, $g^{\mu\nu}$ are the components of the inverse metric such that $g_{\mu\nu} g^{\nu\lambda} = \delta_\mu^\lambda$ (δ_μ^λ is the Kronecker delta), and we have assumed the Einstein summation convention, where like indices are summed over unless otherwise stated. From this point forward, we will not distinguish between the components of a tensor and the tensor itself, i.e. we will call $g_{\mu\nu}$ the metric instead of the components of the metric. Finally, $R = g^{\mu\nu} R_{\mu\nu}$ is the Ricci scalar. Since $R_{\mu\nu}$ and R are made up of second derivatives of the metric, the left-hand side of (2.1) gives information about the curvature of the space, while the right-hand side can be viewed as a source term. This is the statement that energy and momentum curve spacetime [15, 18].

The cosmological constant term can be viewed in two ways: if placed on the left-hand side, it introduces a constant contribution to the curvature everywhere in the space, but when placed on the right-hand side, it adds a constant energy-momentum term everywhere (i.e. a constant vacuum energy-momentum density). The resulting geometry is indifferent to the interpretation of the cosmological constant [15, 18]. We will be mainly focusing on asymptotically Anti-de Sitter spaces for which $\Lambda < 0$.

Tensor equations are used in general relativity due to the fact that tensor equations such as (2.1) are form invariant under coordinate transformations [19]. We often choose coordinates adapted to observers, and so the form invariance of equations under coordinate transformation is the same as requiring that the fundamental laws of physics are the same in all reference frames. In fact, coordinate systems can be thought of as a gauge freedom of general relativity, one that will be thoroughly exploited in this thesis. This becomes quite useful due to the fact that different coordinate systems can give different insights to the

space, and certain coordinates are better adapted to the symmetries of the space.

2.2 Killing Vectors

For reasons which will become clear in later sections, it is important to be able to identify symmetries of the space. We can identify a symmetry of a space as an infinitesimal coordinate transformation, $x^\mu \rightarrow x'^\mu = x^\mu + aK^\mu$, which leaves the metric unchanged, $g_{\mu\nu}(x^\mu) = g_{\mu\nu}(x'^\mu)$.

To find K^μ , we must solve Killing's equations

$$\nabla_{(\mu}K_{\nu)} = \nabla_\mu K_\nu + \nabla_\nu K_\mu = 0 \quad (2.3)$$

where ∇_μ is the covariant derivative

$$\nabla_\mu K_\nu = \partial_\mu K_\nu - \Gamma_{\mu\nu}^\lambda K_\lambda. \quad (2.4)$$

K^μ is called the Killing vector of a space and is often represented in its coordinate-invariant form $\xi = K^\mu \partial_\mu$ [15, 18, 19].

As an example, we can consider \mathbb{R}^2 in polar coordinates, with metric

$$ds^2 = dr^2 + r^2 d\phi^2. \quad (2.5)$$

Notice we have used the differential line element form of the metric, given by $ds^2 = g_{\mu\nu} dx^\mu dx^\nu$.

The non-zero Christoffel symbols are

$$\Gamma_{\phi\phi}^r = -r \quad , \quad \Gamma_{r\phi}^\phi = \Gamma_{\phi r}^\phi = \frac{1}{r} \quad (2.6)$$

and equation (2.4) yields three unique coupled differential equations

$$\begin{aligned} \nabla_r K_r &= \partial_r K_r = 0 \\ \nabla_\phi K_\phi &= \partial_\phi K_\phi + r K_r = 0 \\ \nabla_\phi K_r + \nabla_r K_\phi &= \partial_\phi K_r + \partial_r K_\phi - \frac{2}{r} K_\phi = 0 \end{aligned} \quad (2.7)$$

These equations give three unique solutions

$$\begin{aligned}
K_\mu^{(1)} &= (0, r^2) \Rightarrow (K^{(1)})^\mu = (0, 1) \Rightarrow \xi^{(1)} = \partial_\phi \\
K_\mu^{(2)} &= (\sin \phi, r \cos \phi) \Rightarrow (K^{(2)})^\mu = \left(\sin \phi, \frac{1}{r} \cos \phi \right) \Rightarrow \xi^{(2)} = \sin \phi \partial_r + \frac{1}{r} \cos \phi \partial_\phi \\
K_\mu^{(3)} &= (\cos \phi, -r \sin \phi) \Rightarrow (K^{(3)})^\mu = \left(\cos \phi, -\frac{1}{r} \sin \phi \right) \Rightarrow \xi^{(3)} = \cos \phi \partial_r - \frac{1}{r} \sin \phi \partial_\phi
\end{aligned} \tag{2.8}$$

where we have used the index-raising property of the metric, $K^\mu = g^{\mu\nu} K_\nu$. From the form of $\xi^{(1)}$, we can see that \mathbb{R}^2 has a symmetry of translation in ϕ , or rotational symmetry. However, the interpretations of $\xi^{(2,3)}$ are somewhat obscure. To get a clearer understanding of what these symmetries are, we can define Cartesian coordinates

$$x = r \cos \phi, \quad y = r \sin \phi \Rightarrow r = \sqrt{x^2 + y^2}, \quad \phi = \arctan\left(\frac{y}{x}\right) \tag{2.9}$$

such that the metric becomes

$$ds^2 = dx^2 + dy^2. \tag{2.10}$$

The advantage of writing the Killing vector in its coordinate invariant form is that we can directly apply the coordinate transformation instead of solving Killing's equation again. By the chain rule, we find

$$\begin{aligned}
\partial_r &= \frac{\partial x}{\partial r} \partial_x + \frac{\partial y}{\partial r} \partial_y = \frac{x}{\sqrt{y^2 + x^2}} \partial_x + \frac{y}{\sqrt{y^2 + x^2}} \partial_y \\
\partial_\phi &= \frac{\partial x}{\partial \phi} \partial_x + \frac{\partial y}{\partial \phi} \partial_y = -y \partial_x + x \partial_y
\end{aligned} \tag{2.11}$$

and $\xi^{(2)}$ and $\xi^{(3)}$ become

$$\xi^{(2)} = \partial_y, \quad \xi^{(3)} = \partial_x \tag{2.12}$$

which simply correspond to translations in the y and x directions, respectively. In total, we have found that \mathbb{R}^2 has symmetry of translations in the x and y directions and of rotations in the ϕ direction, which are exactly the symmetries we should expect of 2-dimensional Euclidean space.

2.3 Conformal Killing Vectors

Along with standard Killing vectors, we will be concerned with finding the conformal Killing vectors of a space, which preserve the metric under transformations generated by the vectors, but only up to scale. In other words, under infinitesimal coordinate transformation, $x^\mu \rightarrow x'^\mu = x^\mu + aK^\mu$, the metric in coordinates x'^μ is conformally related to the metric in coordinates x^μ , $g_{\mu\nu}(x^\mu) = \lambda^2 g_{\mu\nu}(x'^\mu)$, where λ^2 is some positive constant. In a spacetime with spatial dimension n , a conformal Killing vector obeys a modified version of Killing's equation [20]

$$\nabla_\mu K_\nu + \nabla_\nu K_\mu - \frac{2}{n} g_{\mu\nu} \nabla_\lambda K^\lambda = 0. \quad (2.13)$$

If the trace of the covariant derivative of K^μ is zero, $\nabla_\lambda K^\lambda = 0$, this simplifies to the standard Killing's equation. As we will see later, conformal Killing vectors are useful for studying symmetries on the boundary of a space.

2.4 Embedding Spaces

Often, the metric on a manifold can be complicated and hard to deal with. For example, consider the metric with non-trivial coordinate dependence

$$ds^2 = d\theta^2 + \sin^2 \theta d\phi^2. \quad (2.14)$$

It may not be immediately obvious what this manifold is describing, but it can be useful to realize it as a submanifold of a higher-dimensional space [21]. If we define the coordinates

$$\begin{aligned} x &= \sin \theta \cos \phi \\ y &= \sin \theta \sin \phi \\ z &= \cos \theta \end{aligned} \quad (2.15)$$

the somewhat complicated metric simply becomes the metric on \mathbb{R}^3

$$ds^2 = dx^2 + dy^2 + dz^2. \quad (2.16)$$

However, since we have gone from a 2-dimensional space to a 3-dimensional one, we must specify a constraint equation to define the original 2-dimensional surface embedded in the 3-dimensional space. In this case, by considering (2.15), we can see that the surface is given by

$$x^2 + y^2 + z^2 = 1 \tag{2.17}$$

and it is now clear that the metric (2.14) is the metric on the unit 2-sphere (Figure 2.1). The benefit of describing (2.14) as a submanifold of \mathbb{R}^3 is that the embedding space is much easier to perform calculations with due to the trivial coordinate dependence. The constraint equation also allows us to find other useful coordinate transformations since any set of coordinates that satisfy (2.17) are valid coordinates on the sphere.

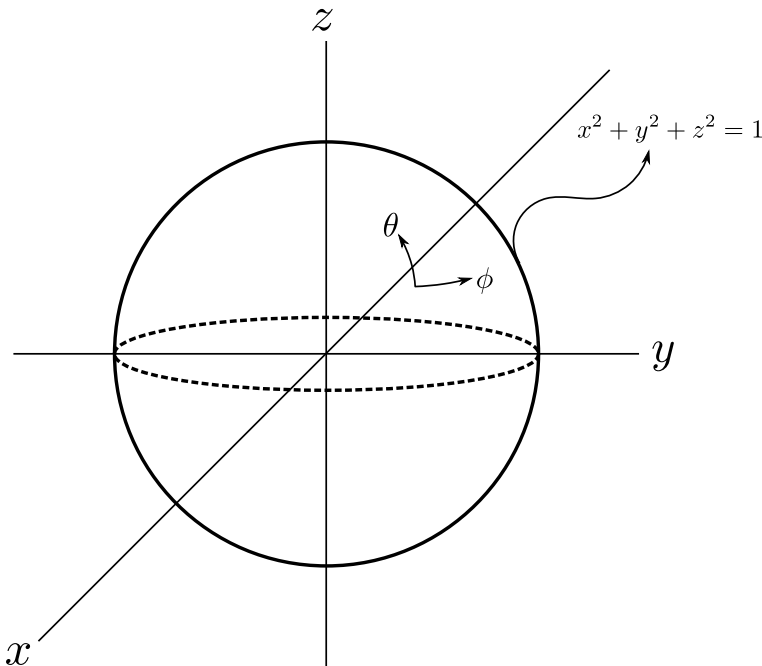


Figure 2.1: The 2-sphere can either be parameterized by two coordinates, θ and ϕ , on the surface itself, or as a submanifold of \mathbb{R}^3 described by the constraint equation $x^2 + y^2 + z^2 = 1$.

While embedding spaces are powerful, we must realize that the submanifold and the embedding space can have very different properties. In this particular example, \mathbb{R}^3 is globally flat, while the sphere has constant curvature everywhere on the surface [18]. We must also

be wary of the fact that the symmetries of \mathbb{R}^3 are not necessarily the same as those of the sphere. For example, since the sphere is uniform, it has a symmetry of translations on its surface. If these translations along the surface of the sphere are represented in the embedding space, they will look like rotations, which are also symmetries of the embedding space. However, translational symmetries of the embedding space will not carry over to the sphere, since these symmetries are orthogonal to the sphere in regions.

We can show this mathematically by considering the Killing vector associated with translations in the x -direction in the embedding space, given by $\xi = \partial_x$. Using the coordinate transformations (2.15), we find that this becomes

$$\xi = -\frac{\sin \phi}{\sin \theta} \partial_\phi \tag{2.18}$$

on the sphere. Using (2.18) and the metric (2.14) in Killing's equation, (2.4), we find $\nabla_{(\mu} K_{\nu)} \neq 0$. Since Killing's equation is not satisfied, ξ cannot generate a symmetry on the sphere, despite the fact that it generates a symmetry of the embedding space. If, however, we choose a rotational symmetry (in this case, a rotation in the $x-y$ plane) of the embedding space, generated by

$$\xi = -y\partial_x + x\partial_y, \tag{2.19}$$

we can transform this into a vector on the sphere, given by

$$\xi = \partial_\phi. \tag{2.20}$$

This vector does satisfy Killing's equation, and we find that the only symmetries of \mathbb{R}^3 which translate to the sphere are the rotations in the three orthogonal planes, as expected. We will be focusing on spaces which have clear representations as subsurfaces in embedding spaces, and we will find it important to identify symmetries of the embedding spaces which carry over to the subsurfaces.

2.5 Anti-de Sitter Spacetime

Global d -dimensional Anti-de Sitter spacetime (AdS_d) is the maximally symmetric solution to Einstein's equations with one timelike direction and $d - 1$ spacelike directions and constant negative curvature. We can realize AdS_d as the d -dimensional hyperbolic surface

$$-T_1^2 - T_2^2 + \sum_{n=1}^{d-1} X_n^2 = -l \quad (2.21)$$

embedded in the $d + 1$ -dimensional Minkowski-like space, $\mathbb{R}^{2,d-1}$, with metric

$$ds^2 = -dT_1^2 - dT_2^2 + \sum_{n=1}^{d-1} dX_n^2 \quad (2.22)$$

where l is known as the Anti-de Sitter radius and is inversely related to the constant curvature of the space [3]. For simplicity, we will set $l = 1$. The coordinate ranges of $\mathbb{R}^{2,d-1}$ are $T_{1,2} \in (-\infty, \infty)$ and $X_n \in (-\infty, \infty)$. A cross-section of AdS_d at $T_2 = X_{n+2} = 0$ is shown in Figure 2.2.

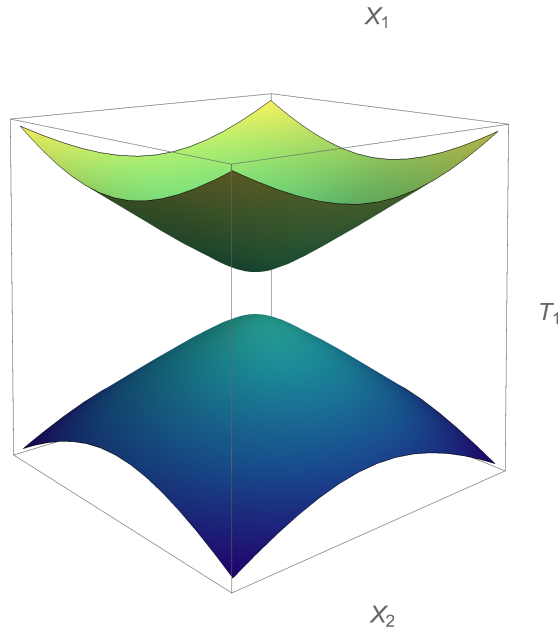


Figure 2.2: Cross section of AdS_d at $T_2 = X_{n+2} = 0$ described by surface (2.21) embedded in $\mathbb{R}^{2,d-1}$.

To study AdS_d , we will define “spherical” coordinates on the surface (2.21) [23]

$$\begin{aligned}
T_1 &= \sqrt{r^2 + 1} \cos t \\
T_2 &= \sqrt{r^2 + 1} \sin t \\
X_n &= rx_n \quad \text{where} \quad \sum_n x_n^2 = 1.
\end{aligned}
\tag{2.23}$$

The x_n 's are shorthand for the angular coordinates, i.e. $x_1 = \sin \phi_1 \sin \phi_2 \dots \cos \phi_{d-2}$, $x_2 = \sin \phi_1 \sin \phi_2 \dots \sin \phi_{d-2}$ etc. The coordinate ranges are given by $t \in (0, 2\pi]$, $r \in [0, \infty)$, $\{\phi_1, \phi_2, \dots, \phi_{d-3}\} \in [0, \pi]$, and $\phi_{d-2} \in (0, 2\pi]$. We notice that the coordinate t , which acts as time in these coordinates, is periodic. This leads to *closed timelike curves*, i.e. trajectories of massive particles which loop back on themselves in time. This is a problem for the causality of the spacetime, since we can no longer specify cause and effect (Figure 2.3) [18]. To remedy this, we enforce a universal covering, which unwraps the time coordinate so that it has the range $t \in (-\infty, \infty)$. We can also see that this coordinate transformation does indeed satisfy (2.21). The metric (2.22) becomes

$$ds^2 = -(r^2 + 1)dt^2 + (r^2 + 1)^{-1}dr^2 + r^2 d\Omega_{d-2}^2
\tag{2.24}$$

where $d\Omega_{d-2}^2$ is the metric on the unit $(d - 2)$ -sphere.

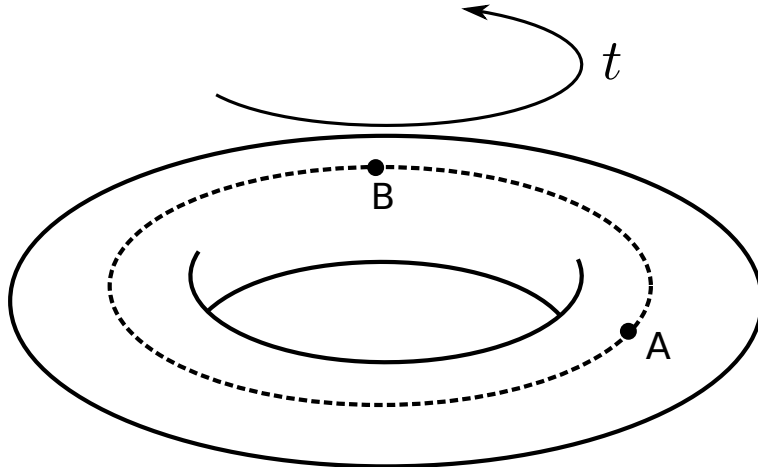


Figure 2.3: Example of how causality is violated with closed timelike curves. If the time coordinate, t , is periodic, we can have trajectories of massive particles (dashed line) which loop back on themselves in time. However, if two causally connected events, A and B, occur on this trajectory, it is impossible to say which caused the other, violating causality.

Light cones of a spacetime, which can be found by setting $ds^2 = 0$, can give insight to the properties of the spacetime. Restricting to radial trajectories, we can suppress $d\Omega_{d-2}^2$ and solve

$$0 = -(r^2 + 1)dt^2 + (r^2 + 1)^{-1}dr^2 \Rightarrow \frac{dt}{dr} = \pm(r^2 + 1)^{-1}$$

$$\Rightarrow t(r) = \pm \arctan r \mp \arctan r_0 \quad (2.25)$$

where r_0 is an initial value of the r -coordinate. These null trajectories are plotted in Figure 2.4.

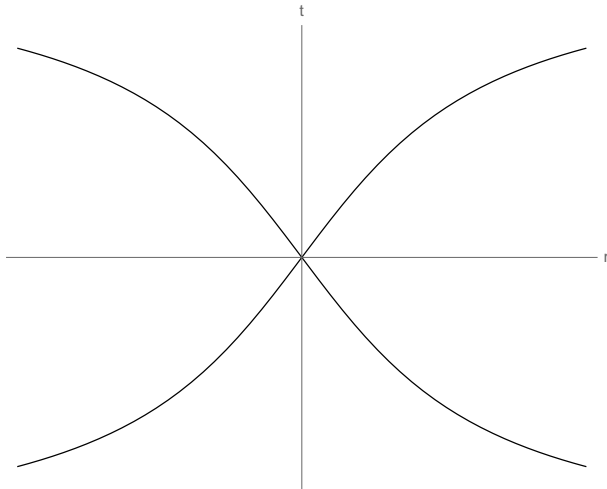


Figure 2.4: Lightlike trajectories for AdS_d in spherical coordinates. These begin at $t = 0$ like those in Minkowski space, but then flatten out as $t \rightarrow \pi/2$.

If we want our light cones to be the standard 45-degree lines we are used to from Minkowski space, we can define a new radial coordinate

$$dr^* = \frac{dr}{r^2 + 1} \Rightarrow r^* = \arctan r \quad (2.26)$$

so that the metric becomes (with angular coordinates suppressed)

$$ds^2 = \sec^2 r^* (-dt^2 + dr^{*2}) \quad (2.27)$$

where $r^* \in (0, \pi/2)$. By setting $ds^2 = 0$, we find $t(r^*) = \pm(r^* - r_0^*)$ and null trajectories are just lines at 45-degrees. However, we have also introduced a new interesting feature of the metric. If we multiply ds^2 by a conformal factor $\Omega^2 = \cos^2 r^*$, such that the angles between null trajectories are preserved, we find

$$d\tilde{s}^2 = \Omega^2 ds^2 = -dt^2 + dr^{*2} \tag{2.28}$$

where $d\tilde{s}^2$ (called the unphysical metric) is just the metric of 2-dimensional Minkowski space [15, 18]. From the coordinate transformation (2.26), we can see that $r \rightarrow \infty$ is mapped to the finite point $r^* = \pi/2$ after the conformal transformation, which is just a timelike line (see Figure 2.5). Since $r = \infty$ is timelike, it means that light can reach $r = \infty$ and return to the origin, $r = 0$, in finite time. In this sense, AdS_d has a boundary, and this asymptotic boundary is exactly the space we use as the background for the CFT in the AdS/CFT correspondence [2, 3].

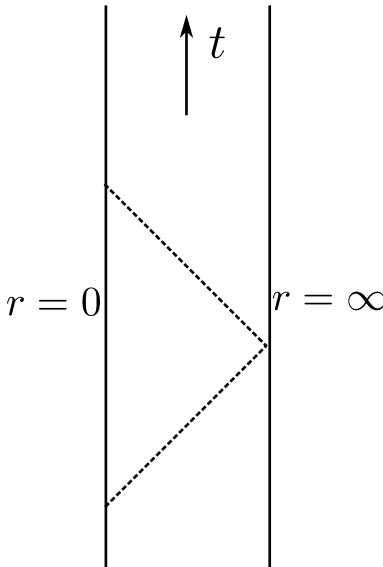


Figure 2.5: Penrose diagram of global AdS with angular coordinates suppressed. The time coordinate runs in the vertical direction and the radial coordinate runs in the horizontal direction. The line on the left represents the origin of the space ($r = 0$) and the line on the right represents infinity ($r = \infty$). The dashed line shows the trajectory of a lightlike particle which reaches infinity and returns to $r = 0$ in finite time.

2.6 Quotients

One interesting aspect of differential geometry is that spaces that are different globally (have different topologies) can look the same locally (have the same curvature). In fact, we can build spaces which have interesting global properties from topologically trivial spaces. One possible way of building these topologically different spaces is by performing a quotient [24]. To quotient a space, we must first identify a symmetry of the space, which is usually done by solving Killing's equation. Then, we cut the space orthogonal to the Killing's vector field, and finally we identify the cuts as the same surface.

For example, take the 2-dimensional Euclidean plane, \mathbb{R}^2 , with metric

$$ds^2 = dx^2 + dy^2. \quad (2.29)$$

This space has a Killing vector, $\xi = \partial_x$, which generates the transformation $(x, y) \rightarrow (x+a, y)$, where a is an arbitrary parameter. Introducing a new coordinate (for reasons which will become clear), $\theta = (2\pi/a)x$, the metric becomes

$$ds^2 = dy^2 + \left(\frac{a}{2\pi}\right)^2 d\theta^2 \quad (2.30)$$

with Killing vector $\xi = (2\pi/a)\partial_\theta$, which now generates the transformation $(\theta, y) \rightarrow (\theta+2\pi, y)$. Since this Killing vector tells us that the surfaces θ and $\theta + 2\pi$ are identical, we can glue these two surfaces together such that $\theta \in (0, 2\pi]$. The space keeps the property of flatness, but since we have taken an infinite coordinate and made it periodic, we have changed the topology of the space from a plane to a cylinder with radius $a/(2\pi)$ (Figure 2.6).

As we have already seen, identifying the exact form of the transformation generated by an arbitrary Killing vector can be significantly more challenging than this simple example with \mathbb{R}^2 , so we may be forced to change coordinates so that the action of the quotient is clear [25].

The act of quotienting a space (especially AdS) is of interest due to the fact that we can obtain interesting, nontrivial spaces from very simple spaces and retain many of the simple properties of the original space.

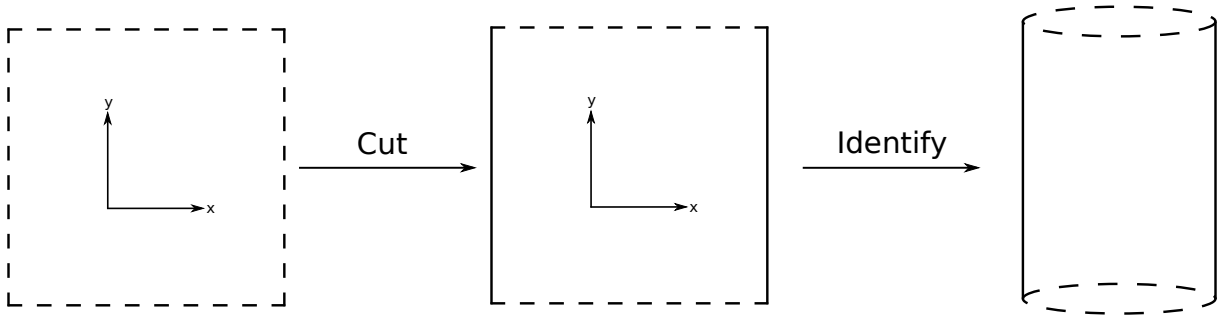


Figure 2.6: The act of quotienting \mathbb{R}^2 to obtain the cylinder. First, we identify that \mathbb{R}^2 has Killing vector associated with translations in x . Then, we cut the space orthogonal to the flow of this Killing vector. Finally, we identify the two cuts to change the topology of the space. Dashed lines extend to infinity in this figure.

2.7 Topological Black Holes: The BTZ Black Hole

To further see the power of quotienting spaces and to set the stage for the main spacetime of interest, we will consider the $(2 + 1)$ -dimensional topological “BTZ” black hole, named after Bañados, Teitelboim, and Zanelli [13]. First, however, it will be helpful to introduce the black hole in asymptotically $(3 + 1)$ -dimensional Minkowski space for comparison. This black hole was discovered by Schwarzschild in 1916 by assuming a spherically symmetric vacuum solution to Einstein’s equation with no cosmological constant [15, 18]. The Schwarzschild metric is given by

$$ds^2 = - \left(1 - \frac{2G_N M}{r} \right) dt^2 + \left(1 - \frac{2G_N M}{r} \right)^{-1} dr^2 + r^2 d\Omega_2^2 \quad (2.31)$$

where M is the mass of the black hole [15, 18]. This form of the metric has two surfaces where the metric is ill-behaved: $r = 2G_N M$ and $r = 0$. However, these pathologies may just be an artifact of coordinates, not an actual problem with the curvature. If we want to study the curvature at these surfaces, we can use the Riemann tensor, defined as

$$R^\mu{}_{\nu\lambda\alpha} = \partial_\lambda \Gamma^\mu_{\nu\alpha} - \partial_\alpha \Gamma^\mu_{\nu\lambda} + \Gamma^\beta_{\nu\alpha} \Gamma^\mu_{\beta\nu\lambda} - \Gamma^\beta_{\nu\lambda} \Gamma^\mu_{\beta\alpha} \quad (2.32)$$

but if these ill-behaved surfaces are a result of coordinates, we need a coordinate-independent quantity, the simplest being a scalar, which we can form by squaring the Riemann tensor

[15, 18]. The square of the Riemann tensor using metric (2.31) is given by

$$R^{\mu\nu\lambda\alpha}R_{\mu\nu\lambda\alpha} = \frac{48G_N^2M^2}{r^2}. \quad (2.33)$$

From this, we see that nothing is diverging in the curvature at $r = 2G_NM$, but we do have diverging curvature at $r = 0$. Since general relativity cannot handle these divergences, we must remove this point from the spacetime, but this creates a surface in spacetime where the trajectories of massive particles can end without reaching infinity. This type of surface is known as a *singularity* [18].

At $r = 2G_NM$, although the curvature is not divergent, the dt^2 and dr^2 terms in (2.31) switch signs, i.e. the spacelike term dr^2 becomes timelike for $r < 2G_NM$. Since massive and lightlike particles are only allowed to travel through timelike dimensions in one direction, a massive or lightlike particle which crosses the $r = 2G_NM$ surface can only go toward the singularity at $r = 0$. We call the surface $r = 2G_NM$ an *event horizon* [18].

We begin the discussion of the topological black hole by defining AdS_3 as the surface

$$-T_1^2 - T_2^2 + X_1^2 + X_2^2 = -1 \quad (2.34)$$

embedded in $\mathbb{R}^{2,2}$ with metric [3]

$$ds^2 = -dT_1^2 - dT_2^2 + dX_1^2 + dX_2^2. \quad (2.35)$$

Using (2.35) in Killing's equation yields ten unique coupled differential equations

$$\begin{aligned} \partial_{T_1}K_{T_1} &= 0, \quad \partial_{T_2}K_{T_2} = 0, \quad \partial_{X_1}K_{X_1} = 0, \quad \partial_{X_2}K_{X_2} = 0 \\ \partial_{T_1}K_{T_2} + \partial_{T_2}K_{T_1} &= 0, \quad \partial_{T_1}K_{X_1} + \partial_{X_1}K_{T_1} = 0, \quad \partial_{T_1}K_{X_2} + \partial_{X_2}K_{T_1} = 0 \\ \partial_{T_2}K_{X_1} + \partial_{X_1}K_{T_2} &= 0, \quad \partial_{T_2}K_{X_2} + \partial_{X_2}K_{T_2} = 0, \quad \partial_{X_1}K_{X_2} + \partial_{X_2}K_{X_1} = 0. \end{aligned} \quad (2.36)$$

Note that any solution for K^μ must solve all ten of these equations simultaneously. We will choose the boost-like solution

$$\xi = -X_1\partial_{T_1} - T_1\partial_{X_1} \quad \Rightarrow \quad \xi^2 = K_\mu K^\mu = T_1^2 - X_1^2 \quad (2.37)$$

to generate the quotient [25, 26]. This Killing vector is allowed to have negative magnitude, $\xi^2 < 0$, and can therefore be timelike. Once we perform the quotient, these regions will result in closed timelike curves, so to preserve causality, we must remove them from the space [13, 25]. However, this will create surfaces where trajectories of massive particles can end without reaching infinity, which we recognize as singularities. The locations of the singularities in these coordinates are given by $T_1^2 - X_1^2 = 0$. Using (2.34), this corresponds to the hyperbola $-T_2^2 + X_2^2 = -1$. Since null trajectories in the $T_2 - X_2$ plane are just given by lines at 45-degrees, another interesting surface to examine is $T_2^2 - X_2^2 = 0$, which describes the null trajectories which bound the singularities. Since, once lightlike or massive particles pass these surfaces, they can only go toward the singularity, we recognize these as event horizons. We know that a quotient must preserve local curvature, and so we see that a quotient by ξ will generate a black hole spacetime which is locally AdS_3 , i.e. which has constant curvature everywhere [13, 25]. These special surfaces are plotted in Figure 2.7.

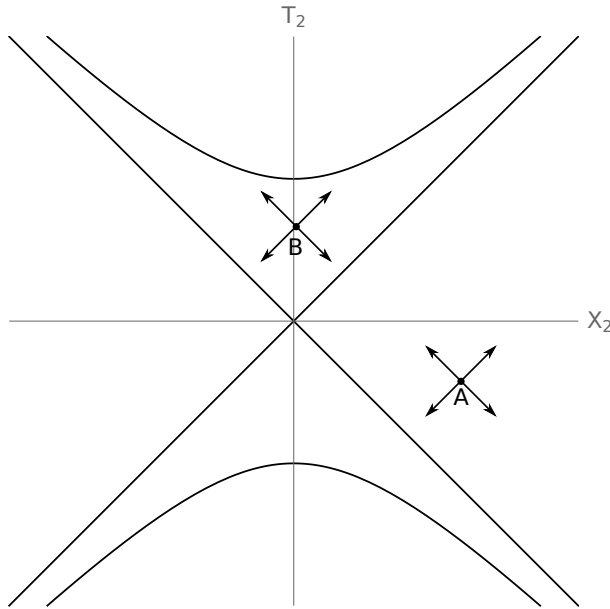


Figure 2.7: Special surfaces induced by a quotient generated by ξ in the $T_2 - X_2$ plane. The hyperbola given by $X_2^2 - T_2^2 = -1$ is the singularity, while the lines $X_2^2 - T_2^2 = 0$ are the event horizons. A and B are spacetime points at which light pulses are emitted in the exterior and interior of the black hole, respectively. The corresponding future-directed and past-directed light cones are 45-degree lines.

To study the topological black hole in more detail, we define coordinates on the surface (2.34) such that ξ generates a spatial translation, $\xi \propto \partial_\phi$. If we choose $T_1 = T_1(r, \phi)$ and $X_1 = X_1(r, \phi)$, then by the chain rule

$$\begin{aligned}\xi &= \left(-X_1 \frac{\partial \phi}{\partial T_1} - T_1 \frac{\partial \phi}{\partial X_1}\right) \partial_\phi + \left(-X_1 \frac{\partial r}{\partial T_1} - T_1 \frac{\partial r}{\partial X_1}\right) \partial_r = \alpha \partial_\phi \\ \Rightarrow -X_1 \frac{\partial \phi}{\partial T_1} - T_1 \frac{\partial \phi}{\partial X_1} &= \alpha, \quad -X_1 \frac{\partial r}{\partial T_1} - T_1 \frac{\partial r}{\partial X_1} = 0\end{aligned}\tag{2.38}$$

where α is an unknown constant. Solving for ϕ , we find

$$\phi = \alpha \operatorname{arctanh}\left(\frac{X_1}{T_1}\right)\tag{2.39}$$

and so we will guess the transformation

$$\begin{aligned}T_1 &= \sqrt{A(r)} \cosh\left(-\frac{\phi}{\alpha}\right) \\ X_1 &= \sqrt{A(r)} \sinh\left(-\frac{\phi}{\alpha}\right)\end{aligned}\tag{2.40}$$

with $A(r)$ an unknown function [25, 26]. We can see that this satisfies the equation in terms of r since we have

$$\begin{aligned}A(r) = T_1^2 - X_1^2 \Rightarrow \frac{\partial}{\partial T_1} [A(r)] &= \frac{\partial A}{\partial r} \frac{\partial r}{\partial T_1} = 2T_1 \Rightarrow \frac{\partial r}{\partial T_1} = \frac{2T_1}{A'}, \\ \frac{\partial}{\partial X_1} [A(r)] &= \frac{\partial A}{\partial r} \frac{\partial r}{\partial X_1} = -2X_1 \Rightarrow \frac{\partial r}{\partial X_1} = -\frac{2X_1}{A'}\end{aligned}\tag{2.41}$$

and so we find

$$-X_1 \frac{\partial r}{\partial T_1} - T_1 \frac{\partial r}{\partial X_1} = -\frac{2X_1 T_1}{A'} + \frac{2T_1 X_1}{A'} = 0.\tag{2.42}$$

Since we are defining coordinates on the subsurface in terms of the embedding space coordinates, the new coordinates must satisfy (2.34). The most natural choice for T_2 and X_2 is

$$\begin{aligned}
T_2 &= \sqrt{B(r)} \sinh(\beta t) \\
X_2 &= \sqrt{B(r)} \cosh(\beta t)
\end{aligned}
\tag{2.43}$$

such that (2.34) becomes

$$-A(r) + B(r) = -1. \tag{2.44}$$

Again, β is an unknown constant to be chosen later. Since now, a symmetry generated by $\xi = \alpha \partial_\phi$ transforms the point $(t, r, \phi) \rightarrow (t, r, \phi + a\alpha)$, we will set $\alpha = 2\pi/a$ so that the quotient will make the ϕ coordinate periodic with range $\phi \in (0, 2\pi]$. In these new coordinates, the metric (2.35) becomes

$$ds^2 = -\beta^2 B(r) dt^2 + \left(\frac{B'(r)^2}{4B(r)} - \frac{A'(r)^2}{4A(r)} \right) dr^2 + \frac{a^2 A(r)}{\pi^2} d\phi^2. \tag{2.45}$$

Once the quotient is made and the ϕ coordinate becomes periodic, we expect the $d\phi^2$ term to be the metric on the 1-sphere, given by $d\Omega_1^2 = r^2 d\phi^2$, and so we choose

$$A(r) = \frac{\pi^2}{a^2} r^2 \Rightarrow B(r) = A(r) - 1 = \frac{\pi^2}{a^2} r^2 - 1 \tag{2.46}$$

so that the metric takes the form

$$ds^2 = -\frac{\beta^2}{a^2} (\pi^2 r^2 - a^2) dt^2 + \left(r^2 - \frac{a^2}{\pi^2} \right)^{-1} dr^2 + r^2 d\phi^2. \tag{2.47}$$

Finally, for simplicity, we set $a = \pi\sqrt{m}$ and $\beta = \sqrt{m}$ and obtain the metric for the BTZ black hole in spherical coordinates

$$ds^2 = -(r^2 - m) dt^2 + (r^2 - m)^{-1} dr^2 + r^2 d\phi^2 \tag{2.48}$$

which has a similar form to (2.31). After the quotient, the coordinate ranges are $t \in (-\infty, \infty)$, $r \in [\sqrt{m}, \infty)$ (since $B(r)$ is constrained to be positive), and $\phi \in (0, 2\pi]$. We can use the coordinate transformations to find the location of the event horizon

$$X_1^2 - T_1^2 = -1 \Rightarrow r = \sqrt{m} \tag{2.49}$$

however, the coordinates are restricted to the exterior of the event horizon, and so do not see the location of the singularity [26]. Since the location of the event horizon depends only on m , we can associate this quantity with the mass of the black hole.

If we want to find coordinates which are valid on the interior of the black hole, we can take $\sqrt{B(r)} \rightarrow -\sqrt{-B(r)}$ in (2.43) and we get back the same metric (2.48) [26]. Here, we can find the location of the singularity

$$X_1^2 - T_1^2 = 0 \Rightarrow r = 0. \quad (2.50)$$

Unfortunately, the metric (2.48) is pathological at the event horizon, but we know that nothing is singular about the curvature there (since this spacetime was formed from a quotient of AdS_3 , it retains the property that the curvature is not coordinate-dependent). To get rid of this pathology, we can define coordinates

$$\begin{aligned} T &= \frac{1}{\sqrt{m}} \left(\frac{r - \sqrt{m}}{r + \sqrt{m}} \right)^{\frac{1}{2}} \sinh(\sqrt{m} t) \\ Z &= \frac{1}{\sqrt{m}} \left(\frac{r - \sqrt{m}}{r + \sqrt{m}} \right)^{\frac{1}{2}} \cosh(\sqrt{m} t) \end{aligned} \quad (2.51)$$

so that the metric becomes

$$ds^2 = \frac{m}{[1 + m(T^2 - Z^2)]^2} [-4dT^2 + 4dZ^2 + (1 + m\{Z^2 - T^2\})^2 d\phi^2] \quad (2.52)$$

which is regular at $r = \sqrt{m}$ or $T = Z = 0$. Due to the coordinate ranges of t and r , $T \in (-\infty, \infty)$, $Z \in [0, \infty)$, and $Z^2 - T^2 \geq 0$, which are again constrained to the exterior of the black hole (Region I in Figure 2.8). If we only consider the metric (2.52) at a constant value of ϕ , we can immediately see that null trajectories are given by 45-degree lines. From the coordinate transformation, it is also clear that the event horizon(s) is (are) located at $Z^2 - T^2 = 0$.

If instead, we want coordinates which are valid on the interior of the black hole, we can use the transformation

$$\begin{aligned}
T &= \frac{1}{\sqrt{m}} \left(\frac{\sqrt{m} - r}{r + \sqrt{m}} \right)^{\frac{1}{2}} \cosh(\sqrt{m} t) \\
Z &= \frac{1}{\sqrt{m}} \left(\frac{\sqrt{m} - r}{r + \sqrt{m}} \right)^{\frac{1}{2}} \sinh(\sqrt{m} t)
\end{aligned}
\tag{2.53}$$

and obtain the metric (2.52). Now, the coordinates are only valid for $T \in [0, \infty)$ and $Z \in (-\infty, \infty)$ (Region II in Figure 2.8). Again, we find the event horizon(s) to be located at $Z^2 - T^2 = 0$.

What is noteworthy about the spacetime we have so far is that it is geodesically incomplete, i.e. we can find null trajectories (past or future directed) that do not end at a singularity or go to infinity [18]. In fact, at the surface $T = -Z$, past-directed null trajectories can end, but we know that this surface is not pathological. To remedy this, we maximally extend the coordinates T and Z so that they always take the ranges $T, Z \in (-\infty, \infty)$ [34]. This process introduces two new regions: a time-reversed version of the black hole, or white hole (Region III in Figure 2.8), and a second exterior region (Region IV in Figure 2.8)! Region IV is asymptotically distinct from Region I (the two regions do not share a boundary), and a particle must propagate superluminally to travel from Region I to Region IV or vice versa. This will be a key difference between the topological black holes in $(2 + 1)$ versus $(3 + 1)$ dimensions.

The BTZ black hole provides a great method for studying black holes due to its simplicity both in the form of the metric (2.48) its coordinate-independent curvature. These characteristics have also made possible many calculations in the AdS/CFT correspondence which would be intractable in other black hole spacetimes [5, 10, 11]. By using the $(3 + 1)$ -dimensional topological black hole, we retain the coordinate-independent curvature, but we must sacrifice another characteristic that makes (2.48) such a convenient metric to perform calculations with: time-independence.

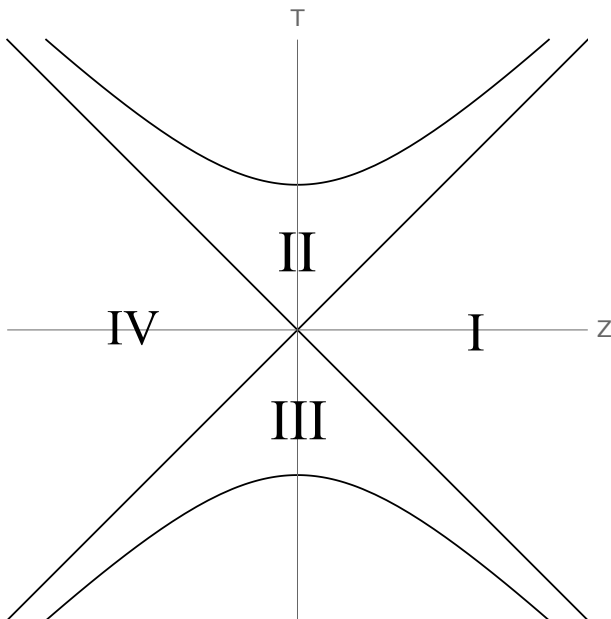


Figure 2.8: Maximally extended BTZ spacetime. Regions I and IV are asymptotically distinct exterior regions, region II is the black hole interior and region III is the white hole interior. This space is geodesically complete since any null geodesic either terminates at a singularity or extends to infinity.

2.8 (3+1)-Dimensional Topological Black Hole

The process of obtaining the topological black hole in (3+1) dimensions is nearly identical to that of section 2.7, but in one higher dimension [14]. We begin with AdS_4

$$-T_1^2 - T_2^2 + X_1^2 + X_2^2 + X_3^2 = -1 \quad (2.54)$$

embedded in $\mathbb{R}^{2,3}$ with metric

$$ds^2 = -dT_1^2 - dT_2^2 + dX_1^2 + dX_2^2 + dX_3^2. \quad (2.55)$$

Like the BTZ case, we can recognize that this space has a boost-like Killing vector $\xi = -X_1\partial_{T_1} - T_1\partial_{X_1}$ which we will choose to generate the quotient [14]. Again, we see that the magnitude $\xi^2 = T_1^2 - X_1^2$ can be timelike, so to avoid closed timelike curves, we remove these regions of the space, and so lightlike or timelike trajectories end at the surface $T_1^2 - X_1^2 = 0$, which we identify as a singularity. From (2.54), we see that this surface corresponds to the hyperboloid $-T_2^2 + X_2^2 + X_3^2 = -1$. This hyperboloid is bounded by the null surface

$-T_2^2 + X_2^2 + X_3^2 = 0$ which, like the BTZ case, we will identify as the event horizon after the quotient. These surfaces are shown in Figure 2.9 [14].

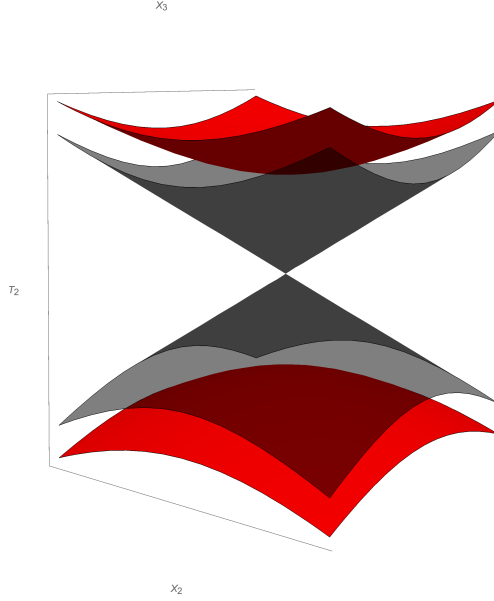


Figure 2.9: Special surfaces induced by a quotient generated by ξ in the $T_2 - X_2 - X_3$ hyperplane. The hyperboloid given by $X_2^2 + X_3^2 - T_2^2 = -1$ is the singularity (red), while the cones $X_2^2 + X_3^2 - T_2^2 = 0$ are the event horizons (black).

To examine the specific behavior of the $(3 + 1)$ -dimensional topological black hole, we must define coordinates on the surface (2.54). We will consider three coordinate systems adapted to different observers that will be important for examining observer-dependence in the AdS/CFT correspondence: the first system is adapted to observers falling into the black hole, the second system corresponds to observers who remain outside of the black hole and see the full exterior as well as a time-dependent spacetime, and the final system corresponds to observers who remain outside of the black hole, but only see a part of the exterior which is time-independent. As in section 2.7, we will choose coordinates where $\xi = \partial_\phi$ is spacelike [14].

The first set of coordinates which are adapted to infalling observers can be given by

$$T_1 = \frac{1 - t^2 + y_1^2 + y_2^2}{1 + t^2 - y_1^2 - y_2^2} \cosh(\phi) \quad , \quad T_2 = \frac{2t}{1 + t^2 - y_1^2 - y_2^2}$$

$$X_1 = \frac{1 - t^2 + y_1^2 + y_2^2}{1 + t^2 - y_1^2 - y_2^2} \sinh(\phi) \quad , \quad X_2 = \frac{2y_1}{1 + t^2 - y_1^2 - y_2^2} \quad , \quad X_3 = \frac{2y_2}{1 + t^2 - y_1^2 - y_2^2}$$
(2.56)

so that the metric (2.55) becomes

$$ds^2 = \frac{4}{(1 + t^2 - y_1^2 - y_2^2)^2} (-dt^2 + dy_1^2 + dy_2^2) + \left(\frac{1 - t^2 + y_1^2 + y_2^2}{1 + t^2 - y_1^2 - y_2^2} \right)^2 d\phi^2$$
(2.57)

where the coordinates take the ranges $t \in (-\infty, \infty)$, $y_1, y_2 \in (-\infty, \infty)$, and $\phi \in (0, 2\pi]$ after the quotient [14]. For convenience later on, it will be helpful to define $y_1 = \chi \cos \theta$ and $y_2 = \chi \sin \theta$, so the metric takes the form

$$ds^2 = \frac{4}{(1 + t^2 - \chi^2)^2} (-dt^2 + d\chi^2 + \chi^2 d\theta^2) + \left(\frac{1 - t^2 + \chi^2}{1 + t^2 - \chi^2} \right)^2 d\phi^2$$
(2.58)

with $\chi \in [0, \infty)$ and $\theta \in (0, 2\pi]$. In these coordinates, the singularity is located at $\chi^2 = t^2 - 1$ and the event horizon is located at $\chi^2 = t^2$. From this, it is clear that the metric (2.58) is regular at the event horizon and therefore is valid over the whole spacetime. At the surface $\chi^2 - t^2 = 1$, the metric diverges, but we see that this surface also corresponds to where the embedding coordinates diverge, and so we identify this surface as the boundary of the spacetime. This spacetime is also geodesically complete since any lightlike trajectory either reaches the boundary or ends at the singularity. Therefore, no maximal extension is necessary and we conclude this spacetime has a single asymptotic boundary, as opposed to the BTZ case, which had two distinct asymptotic boundaries. We will refer to these coordinates as ‘‘Kruskal’’ coordinates, since they are analogous to the maximally extended black hole coordinates originally discovered by Kruskal [18, 34].

The second set of coordinates we will use are given by

$$\begin{aligned}
t &= \rho \sinh \tau \\
y_1 &= \rho \cos \theta \cosh \tau \\
y_2 &= \rho \sin \theta \cosh \tau
\end{aligned} \tag{2.59}$$

with ranges $\tau \in (-\infty, \infty)$, $\rho \in [0, 1)$, and $\theta \in (0, 2\pi]$ [14]. The metric (2.57) becomes

$$ds^2 = \frac{4}{(1 - \rho^2)^2} (-\rho^2 d\tau^2 + d\rho^2 + \rho^2 \cosh^2 \tau d\theta^2) + \left(\frac{1 + \rho^2}{1 - \rho^2} \right)^2 d\phi^2. \tag{2.60}$$

These coordinates do not cover the entire spacetime and in fact are restricted to the region

$$y_1^2 + y_2^2 - t^2 = \rho^2 \geq 0 \tag{2.61}$$

which we can recognize as the exterior of the black hole. We also can see that the boundary is located at $\rho = 1$ where the metric (2.60) diverges. Since these coordinates are valid over the entire exterior, we will refer to them as “full exterior” coordinates. Metric (2.60) is most analogous to (2.48) for the $(2 + 1)$ -dimensional case, but we also note that, since τ plays the role of time, (2.60) is time-dependent while (2.48) does not depend on time.

We can choose instead to work in static coordinates, defined by

$$\begin{aligned}
t &= \rho \sin \psi \sinh \tau \\
y_1 &= \rho \sin \psi \cosh \tau \\
y_2 &= \rho \cos \psi
\end{aligned} \tag{2.62}$$

with $\tau \in (-\infty, \infty)$, $\rho \in [0, 1)$, and $\psi \in [0, \pi]$ [14]. This takes the metric (2.57) to

$$ds^2 = \frac{4}{(1 - \rho^2)^2} (-\rho^2 \sin^2 \psi d\tau^2 + d\rho^2 + \rho^2 d\psi^2) + \left(\frac{1 + \rho^2}{1 - \rho^2} \right)^2 d\phi^2 \tag{2.63}$$

where again, the event horizon is located at $\rho = 0$ and the boundary at $\rho = 1$. While these coordinates have the benefit of being time-independent, they do not cover even the full exterior and are restricted to the region [14]

$$y_1^2 - t^2 \geq 0. \tag{2.64}$$

In this section, we have introduced three coordinate systems which describe the $(3 + 1)$ -dimensional topological black hole spacetime. Kruskal coordinates (2.57), which are time-dependent and exhibit a time-dependent event horizon, full exterior coordinates (2.60), which are also time-dependent, but see a time-independent event horizon, and static coordinates (2.63), which are time-independent, but only cover a portion of the exterior of the black hole.

As we have already seen, general relativity allows for different observers to experience the same spacetime in different ways [15, 18, 33]. However, as we will see, Kruskal and full exterior observers disagree on the area of the event horizon of the black hole and this will have important implications for the discussion of entropy and thermodynamics. This type of disagreement can be seen in comparing accelerated and inertial observers in AdS, but in that context, the different observers are associated with different regions of the boundary theory [17, 31]. In the case of observers corresponding to coordinates (2.57) and (2.60), both are associated with the full boundary and therefore are suitable choices for dual theories to the full CFT. Our goal is to examine how this disagreement between valid choices of coordinates in the bulk is reflected in the boundary CFT.

CHAPTER 3

HOLOGRAPHIC ENTANGLEMENT ENTROPY

The holographic entanglement entropy (HEE) conjecture was originally proposed by Ryu and Takayanagi in 2006 [10]. This was later extended to the covariant prescription of Hubeny, Rangamani, and Takayanagi in 2007 [11]. To introduce HEE, we first motivate the discussion by relating classical entropy to information (or lack thereof) in section 3.1. Then, we introduce the notion of entanglement entropy of quantum systems in section 3.2 and generalize this to local quantum field theories in section 3.3. In section 3.4, we show two ways of calculating entropy of spacetimes: first, by calculating the area of horizons in the spacetime and second, by using a semiclassical approach by defining an action and relating it to the partition function. Finally, we introduce the holographic entanglement entropy conjecture of Ryu-Takayanagi and present known results showing validity of the conjecture.

3.1 Classical Entropy

Perhaps the most relevant way to think of entropy is as a measurement of what an observer can know, but chooses not to. According to statistical mechanics, the entropy of a system is given by

$$S = -k_B \sum_{i=1}^N p_i \log p_i \quad (3.1)$$

where k_B is Boltzmann's constant, N is the total number of possible microstates, and p_i is the probability of the system being in microstate i [27]. This statistical definition of entropy lends itself well to the idea that entropy gives a measurement of what is unknown. For example, if we have a confined gas of particles, we can measure macroscopic quantities of the system, e.g. T , V , N , but the system can still occupy many different states corresponding to microscopic quantities (position, momenta, etc. of each particle). Since each of these states has a probability of occupation, $p_i \neq 1$, we will measure $S \neq 0$ by (3.1). However, if we

choose to know everything about the system, i.e. measure all of the microscopic quantities of every particle, the system will only occupy a single state with $p = 1$ and we will find $S = 0$.

Although the idea of entropy in terms of “intentional ignorance” comes from the classical definition, it naturally extends to both the quantum and relativistic cases.

3.2 Entanglement Entropy

In addition to ordinary thermal entropy, quantum systems can exhibit a new type of entropy, known as entanglement entropy. Given a quantum system described by the density matrix ρ , the von Neumann entropy is given by [28]

$$S = -\text{Tr}(\rho \log \rho). \quad (3.2)$$

The density matrix can be diagonalized such that it is expressed as an ensemble of outer products of state vectors, $\rho = \sum_i c_i |\psi_i\rangle \langle \psi_i|$, where the c_i 's are eigenvalues of the density matrix that can be interpreted as probabilities such that $\sum_i c_i = 1$. If the system can be reduced to a single outer product (i.e. the system can be described by a single state vector), then $S = 0$ and we refer to the state as *pure*; otherwise, we refer to the system as being in a *mixed* state for which $S \neq 0$. However, it is always possible to take a system in a mixed state and realize it as a subsystem of a larger system which itself is in a pure state. The larger system is then referred to as the *purification* of the system in a mixed state. A key feature of the purification is that the original system is non-trivially entangled with the remainder of the larger system [28].

Turning this logic around, we can start with a system in a pure state with vanishing entropy. Then it is possible that considering only a subsystem can give rise to non-trivial entanglement and therefore non-zero entropy for the subsystem. Note, this is in stark contrast to entropy in thermodynamic systems where the entropy of a subsystem of a zero entropy system will always itself be zero [17].

As an example, consider a system consisting of two particles A and B in the spin state

$$|\psi\rangle = \frac{1}{\sqrt{2}} (|\uparrow\downarrow\rangle + |\downarrow\uparrow\rangle) \quad (3.3)$$

where we have used the shorthand notation $|\uparrow\downarrow\rangle = |\uparrow\rangle_A \otimes |\downarrow\rangle_B$ and $|\uparrow\rangle_A$ refers to particle A being in the spin-up state. We can define the density matrix as

$$\rho = |\psi\rangle\langle\psi| \quad (3.4)$$

which is the diagonal form of the density matrix. To find the von Neumann entropy of the total state, we can use the non-zero eigenvalues λ_i

$$S = -\text{Tr}(\rho \log \rho) = -\sum_i \lambda_i \log \lambda_i. \quad (3.5)$$

Since the density matrix (3.4) has only a single non-zero eigenvalue, $\lambda = 1$, we find $S = 0$ and the total state is pure. However, we can restrict our attention to just particle A by tracing over the states of particle B to find the reduced density matrix for particle A

$$\begin{aligned} \rho_A &= \sum_{\alpha=\uparrow,\downarrow} {}_B\langle\alpha|\rho|\alpha\rangle_B \\ &= \frac{1}{2} {}_B\langle\uparrow|(|\uparrow\rangle_A |\downarrow\rangle_B + |\downarrow\rangle_A |\uparrow\rangle_B)(\langle\uparrow|_A \langle\downarrow|_B + \langle\downarrow|_A \langle\uparrow|_B)|\uparrow\rangle_B \\ &\quad + \frac{1}{2} {}_B\langle\downarrow|(|\uparrow\rangle_A |\downarrow\rangle_B + |\downarrow\rangle_A |\uparrow\rangle_B)(\langle\uparrow|_A \langle\downarrow|_B + \langle\downarrow|_A \langle\uparrow|_B)|\downarrow\rangle_B \\ &= \frac{1}{2} (|\uparrow\rangle\langle\uparrow| + |\downarrow\rangle\langle\downarrow|)_A \end{aligned} \quad (3.6)$$

where the final expression is only in terms of particle A and we have used the fact that ${}_B\langle\alpha|\beta\rangle_B = \delta_{\alpha\beta}$ with $\alpha, \beta \in \{\uparrow, \downarrow\}$. Again, this reduced density matrix is in diagonal form, however, ρ_A has two eigenvalues $\lambda_1 = \lambda_2 = 1/2$. Therefore, the von Neumann entropy of just particle A is $S_A = \log 2$ and we can say that particle A is in a mixed state.

We can also consider being given a particle in mixed state (3.6). We can then realize that the combination of ρ_A and ρ_B , $\rho = \rho_A \otimes \rho_B$, is pure. The state ρ would then be considered a purification of state ρ_A .

3.3 Entanglement Entropy in QFTs

The expression for von Neumann entropy (3.2) naturally extends to systems in quantum field theories. If we have a QFT on a manifold $\partial\mathcal{M}$ (a notation which will become clear

in the context of the AdS/CFT correspondence), instead of considering a subsystem, we consider a subregion, A , of $\partial\mathcal{M}$. Generally, the field theory on A will be entangled with the field theory on the rest of $\partial\mathcal{M}$, a region which we will call \bar{A} (Figure 3.1). Just like before, if we define the state of the total QFT on $\partial\mathcal{M}$ as $|\Psi\rangle$, the density matrix of the entire theory is given by [11, 12]

$$\rho_{tot} = |\Psi\rangle\langle\Psi|. \quad (3.7)$$

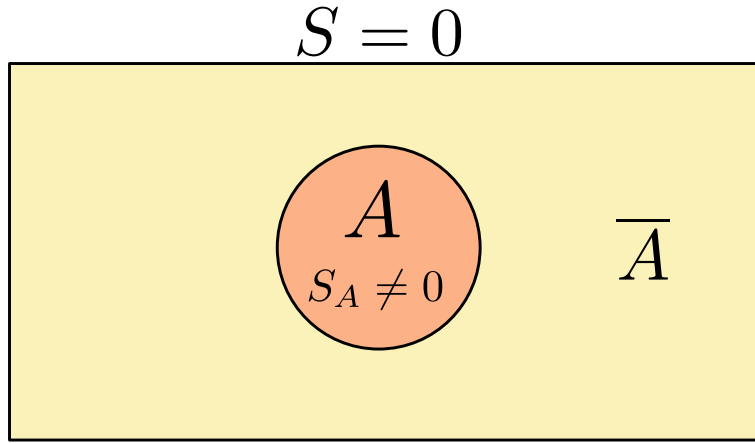


Figure 3.1: QFT on subregion A is entangled with the rest of QFT on \bar{A} and therefore the entanglement entropy for region A is nonzero. Since the total QFT is pure, the entanglement entropy of QFT on $A \cup \bar{A}$ is zero.

We can therefore find the reduced density matrix of the QFT on region A by tracing over the possible states of the QFT on region \bar{A}

$$\rho_A = \text{Tr}_{\bar{A}}(\rho_{tot}) \quad (3.8)$$

then the entanglement entropy of the region A is given by the regular von Neumann entropy

$$S_A = \text{Tr}_A(\rho_A \log \rho_A). \quad (3.9)$$

Unfortunately, the calculation of ρ_{tot} and ρ_A is quite involved for all but the simplest examples [11, 12]. For the special case of the $(1 + 1)$ -dimensional CFT, there exists a formula to calculate entropy introduced by Cardy, given by

$$S = 2\pi\sqrt{\frac{c}{6}\left(L_0 - \frac{c}{24}\right)} \quad (3.10)$$

where L_0 is the product of the energy of the CFT and the length of the region of the CFT that is of interest, and c is the central charge of the CFT (the Noether charge corresponding to an operator which commutes with all other symmetry operators) [29, 40, 43]. Due to the nature of taking the continuum limit of a CFT, many of these calculations diverge and in these cases, it is necessary to regularize the result by introducing a lattice spacing, ϵ , where we take $\epsilon \rightarrow 0$ in the continuum limit [11, 12]. Two important results from the Cardy formula are the entropy of a region A of length $2R$ of a $(1 + 1)$ -dimensional CFT at zero temperature

$$S_A \sim \frac{c}{3} \log \left(\frac{2R}{\epsilon} \right) \quad (3.11)$$

and the entropy of a similar region at finite inverse temperature, β [11, 12]

$$S_A(\beta) \sim \frac{c}{3} \log \left(\frac{\beta}{\pi\epsilon} \sinh \left(\frac{\pi R}{\beta} \right) \right). \quad (3.12)$$

As we will see, these two results (as well as others) serve as a consistency check against the results of the holographic calculation.

Since local QFTs have an infinite number of free parameters in the continuum limit, the entanglement entropy of a subregion of the QFT provides a useful way of determining the free parameters which actively participate in dynamics of the theory. Holographic entanglement entropy seeks to provide another means of simplifying the complex entanglement entropy calculation by relating it to the relatively simple calculation of areas in the bulk.

3.4 Spacetime Entropy

At first, we might not expect black holes to have an intrinsic entropy associated with them since, classically, they are uniquely described by their mass, charge, and angular momentum. However, if we allow a system with nonzero entropy to fall into the black hole, and the black hole itself does not have an entropy observable by an exterior frame, this would violate the second law of thermodynamics: the entropy of the system would be lost to the outside universe when it crosses the horizon. Therefore, a black hole must have a quantity associated

with entropy that can be measured by an outside observer. This entropy can be calculated in two ways: the first, by realizing the close relationship between the area of event horizons and entropy while the second incorporates a semiclassical calculation of the partition function from the action.

3.4.1 Area-Law

If we examine the first law of ordinary thermodynamics,

$$\delta E = T\delta S + P\delta V, \quad (3.13)$$

we see a single term which is necessarily non-decreasing: $\delta S \geq 0$ [27, 35]. On the other hand, a change in energy of a black hole can be given by what is known as the “first law of black hole mechanics”

$$\delta E = \frac{\kappa}{2\pi}\delta A + \Omega\delta J + \Phi\delta Q, \quad (3.14)$$

where κ is the surface gravity at the event horizon, A is the area of the event horizon, Ω is the angular velocity of the horizon, J is the angular momentum of the black hole, Φ is the electric potential, and Q is the charge of the black hole [6]. Classically, a black hole’s angular momentum and charge can increase or decrease, but it has been shown that the area of a black hole’s event horizon is non-decreasing: $\delta A \geq 0$ (known as the “second law of black hole mechanics”) [6, 7]. These results led Bekenstein to propose that the entropy of a black hole is proportional to the area of the event horizon. Hawking later confirmed this and found the proportionality constant to be $1/4G_N$,

$$S_{BH} = \frac{\text{Area}(r = r_s)}{4G_N}, \quad (3.15)$$

where $\text{Area}(r = r_s)$ denotes the area of the event horizon (when the radial component is equal to the Schwarzschild radius), and G_N is Newton’s gravitational constant [8, 9].

In ordinary thermodynamics, entropy is an extensive quantity, meaning that if we take two isolated subsystems and combine them, the entropy of the total system will be the sum of the entropies of the subsystems. Since volumes also display this same additive

characteristic, we say that entropy admits *volume scaling*: the entropy of a system will change proportionally to the volume of the system. This is in contrast to the *area scaling* of black hole entropy. However, it makes sense that the entropy of a black hole scales with the area of the horizon rather than the volume, since an exterior observer cannot gain information about the internal geometry of the black hole, and so it is impossible to calculate the volume. The area scaling of black hole entropy was the first instance of the *holographic nature of gravity*, where information in a spacetime or a region of a spacetime is encoded on the lower-dimensional boundary of the region.

As an example of the area-law for the entropy of black holes, we will examine the BTZ black hole with metric

$$ds^2 = -(r^2 - m)dt^2 + (r^2 - m)^{-1}dr^2 + r^2d\phi^2 \quad (3.16)$$

with coordinate ranges $t \in (-\infty, \infty)$, $r \in (0, \infty)$, and $\phi \in (0, 2\pi]$ and m the mass of the black hole. The area of the event horizon is given by

$$\text{Area}(r = r_s) = \int dx \sqrt{h(r = r_s)} \quad (3.17)$$

where $h(r = r_s)$ is the determinate of the induced metric on the event horizon, located at $r_s = \sqrt{m}$, and x is the coordinate which parameterizes the event horizon [18]. It is noteworthy that, since this is a $(2 + 1)$ -dimensional spacetime, the area calculation actually corresponds to the length of a line. In general, when we calculate the area, we evaluate (3.17) for a $(d - 2)$ -dimensional surface parameterized by $(d - 2)$ coordinates. This induced metric is given by

$$d\sigma_{r=\sqrt{m}}^2 = m d\phi^2. \quad (3.18)$$

Taking the determinate gives

$$h(r = 2m) = m. \quad (3.19)$$

This gives the expression for the area of the event horizon

$$\text{Area}(r = 2m) = \sqrt{m} \int_0^{2\pi} d\phi = 2\pi\sqrt{m}. \quad (3.20)$$

Therefore, by using (3.15), we find the entropy of the BTZ black hole to be

$$S_{BH} = \frac{\pi\sqrt{m}}{2G_N} \quad (3.21)$$

and we see that the entropy of the black hole grows proportionally with the square root of the mass of the black hole.

In comparing the first law of black hole mechanics (3.14) to the first law of thermodynamics (3.13), we can also see that, if area is related to entropy, then the coefficient of δA in (3.14) should be related to temperature. In fact, Hawking found that the temperature of the black hole can be given directly in terms of the surface gravity at the event horizon by

$$T = \frac{\kappa}{2\pi} \quad (3.22)$$

where the surface gravity is given by

$$K^\mu \nabla_\mu K^\nu = \kappa K^\nu \quad (3.23)$$

where K^μ is the Killing vector which becomes null at the event horizon [6, 18]. We can calculate the temperature of the BTZ black hole by solving for κ in equation (3.23) evaluated at the event horizon. However, the metric (2.48) is not well behaved at the event horizon $r = \sqrt{m}$, so we define a new time coordinate

$$v = t + \int \frac{dr}{r^2 - m} \quad (3.24)$$

so that the metric

$$ds^2 = -(r^2 - m)dv^2 + 2dvdr + r^2d\phi^2 \quad (3.25)$$

is regular at $r = \sqrt{m}$. We find that this spacetime has a Killing vector $\xi = \partial_v$ which has magnitude

$$\xi^2 = K^\mu K_\mu = -(r^2 - m) \quad (3.26)$$

which is null at the event horizon $r = \sqrt{m}$. The v -component of equation (3.23) gives

$$r = \kappa. \quad (3.27)$$

Evaluated at $r = \sqrt{m}$, we find the temperature of the BTZ black hole to be

$$T = \frac{\sqrt{m}}{2\pi}. \quad (3.28)$$

These definitions of entropy and temperature have been historically important in defining Hawking radiation and the process of black hole evaporation [8, 32]. However, since they rely on event horizons in the spacetime, they can be difficult to interpret in cases such as thermal AdS or cases where event horizons change according to observers. For these special cases, we can use a semiclassical approach to find these quantities.

3.4.2 Semiclassical Thermodynamic Calculations

The driving force behind spacetime thermodynamics from a semiclassical approach is the Wick rotation. The Wick rotation realizes the fact that, in a Lorenzian-signature space, if we take the time coordinate to be imaginary, it becomes a Euclidean-signature space [44]. For example, take the BTZ metric in spherical coordinates. If we take $t \rightarrow -it_E$, the metric (2.48) becomes

$$ds^2 = (r^2 - m)dt_E^2 + (r^2 - m)^{-1}dr^2 + r^2d\phi^2 \quad (3.29)$$

which has Euclidean signature (all terms positive) for $r > \sqrt{m}$. In quantum mechanics, the time evolution operator is given by (for time-independent Hamiltonian, \hat{H}) [28]

$$\hat{U} = \exp(-i\hat{H}t). \quad (3.30)$$

If the Hamiltonian has an eigenbasis

$$\hat{H}|\psi_n\rangle = E_n|\psi_n\rangle \quad (3.31)$$

where E_n is the energy of the $|\psi_n\rangle$ state, we can re-write the time-evolution operator as [28]

$$\hat{U} = \sum_{m,n} |\psi_m\rangle \langle \psi_m| \exp(-i\hat{H}t) |\psi_n\rangle \langle \psi_n| = \sum_n |\psi_n\rangle \exp(-iE_n t) \langle \psi_n|. \quad (3.32)$$

Taking $t \rightarrow -it_E$, the time evolution operator becomes

$$\hat{U}_E = \sum_n |\psi_n\rangle \exp(-E_n t_E) \langle \psi_n| \quad (3.33)$$

which takes a near identical form to the partition function

$$Z = \sum_n \exp(-\beta E_n) \quad (3.34)$$

where β is the inverse temperature [27, 35]. Clearly, the Euclidean time and inverse temperature are closely related, and since Green's functions (and therefore propagators which use the time evolution operator to propagate a state) are periodic in imaginary time with period β , we can calculate the temperature of a spacetime by finding the periodicity of the Euclidean time coordinate [16].

Using (3.29), we can find the periodicity of t_E by looking near the origin, $r = \sqrt{m}$, of the Euclidean signature space. This limit is given by

$$r = \sqrt{m}(1 + \epsilon^2), \quad 0 < \epsilon \ll 1 \Rightarrow dr = 2\sqrt{m}\epsilon d\epsilon, \quad r^2 - m = 2m\epsilon^2 + O(\epsilon^4) \quad (3.35)$$

and so the metric (3.29) becomes

$$\begin{aligned} ds^2 &= 2m\epsilon^2 dt_E^2 + 2d\epsilon^2 + m(1 + 2\epsilon^2)d\phi^2 + O(\epsilon^4) \\ \Rightarrow ds^2 &= 2[m\epsilon^2 dt_E^2 + d\epsilon^2] + m(1 + 2\epsilon^2)d\phi^2 + O(\epsilon^4). \end{aligned} \quad (3.36)$$

The term in square brackets we can recognize as the metric on a disk

$$ds_{disk}^2 = dr^2 + r^2 d\theta^2 \quad (3.37)$$

if t_E has periodicity

$$\beta = \frac{2\pi}{\sqrt{m}} \quad (3.38)$$

and so the temperature is given by

$$T = \frac{1}{\beta} = \frac{\sqrt{m}}{2\pi} \quad (3.39)$$

which is the exact result from the surface gravity calculation. Note that, to find the temperature using the periodicity trick, we had to take the near-horizon limit. Because of this, we conclude that the black hole is radiating at temperature T . This is not always the case: it is possible that we do not need to take this limit to obtain a periodic Euclidean time and can conclude that the entire space is at temperature T [16].

The semiclassical method of calculating the entropy of a spacetime is more involved than the area calculation. If we specify a gravitational action I_E , we can define the partition function [16]

$$Z = e^{-I_E} \tag{3.40}$$

and the entropy will be given by [16, 27, 35]

$$S = (1 - \beta \partial_\beta) \log Z. \tag{3.41}$$

We can begin with the Einstein-Hilbert action, from which the equations of motion of (Euclidean) general relativity (2.1) can be derived

$$I_{EH} = -\frac{1}{16\pi G_N} \int d^d x \sqrt{g} (R - 2\Lambda) \tag{3.42}$$

where g is the determinate of the Euclidean signature metric, R is the Ricci scalar and Λ is the cosmological constant [16, 18]. For the case of the BTZ black hole, these take the values

$$\sqrt{g} = r \quad , \quad R = -6 \quad , \quad \Lambda = -1 \tag{3.43}$$

and the Einstein-Hilbert action can be evaluated

$$I_{EH} = \frac{1}{4\pi G_N} \int_0^\beta dt_E \int_{\sqrt{m}}^{r_\infty} dr r \int_0^{2\pi} d\phi = \frac{\beta}{4G_N} (r_\infty - m) \tag{3.44}$$

where r_∞ is a cutoff such that, in the limit where $r_\infty \rightarrow \infty$, the action diverges. To remedy this, we can add a counter-term to the action to cancel off the divergent term in the form of the Gibbons-Hawking-York boundary term

$$I_{GHY} = -\frac{1}{8\pi G_N} \int d^{d-1} x \sqrt{h} (K + L_{ct}[h]) \tag{3.45}$$

where h is the determinate of the induced metric on r_∞ , K is the trace of the extrinsic curvature of the boundary and $L_{ct}[h]$ is a function of the induced metric yet to be determined [16, 45]. We are allowed to add this term to the action since it is only a function of h and will not change the equations of motion for a variation in $g_{\mu\nu}$. The induced metric at constant r is given by

$$d\sigma^2 = (r^2 - m)dt_E^2 + r^2d\phi^2 \quad (3.46)$$

and the determinate evaluated at $r = r_\infty$ is given by

$$\sqrt{h} = r_\infty \sqrt{r_\infty^2 - m}. \quad (3.47)$$

We can define a normal vector, n^μ to the surface described by $h_{\mu\nu}$ by

$$h_{\mu\nu} = g_{\mu\nu} - n_\mu n_\nu \quad (3.48)$$

and in this particular case, we find only a single non-zero component of n_μ [11, 18]

$$n_r = -(r^2 - m)^{\frac{1}{2}}. \quad (3.49)$$

We can define the trace of the extrinsic curvature in terms of this normal vector [11, 18]

$$K = \nabla_\mu n^\mu. \quad (3.50)$$

Evaluated at $r = r_\infty$, this gives

$$K = -r_\infty (r_\infty^2 - m)^{-\frac{1}{2}} - \frac{1}{r_\infty} (r_\infty^2 - m)^{\frac{1}{2}}. \quad (3.51)$$

Using this expression in (3.45), we find

$$I_{GHY} = -\frac{1}{8\pi G_N} \int_0^\beta dt_E \int_0^{2\pi} d\phi \left[r_\infty \sqrt{r_\infty^2 - m} \left(-r_\infty (r_\infty^2 - m)^{-\frac{1}{2}} - \frac{1}{r_\infty} (r_\infty^2 - m)^{\frac{1}{2}} + L[h] \right) \right]. \quad (3.52)$$

If we choose $L[h] = c$ where c is a constant, this becomes

$$I_{GHY} = \frac{\beta}{4G_N} \left(2r_\infty^2 - m - c r_\infty \sqrt{r_\infty^2 - m} \right). \quad (3.53)$$

Since we are taking the limit as $r_\infty \rightarrow \infty$, the square root term can be expanded in terms of $1/r_\infty$

$$c r_\infty \sqrt{r_\infty^2 - m} = c r_\infty^2 \sqrt{1 - \frac{m}{r_\infty^2}} = c \left(r_\infty^2 - \frac{m}{2} \right) + O\left(\frac{1}{r_\infty^2}\right) \quad (3.54)$$

and the Gibbons-Hawking-York boundary term is

$$I_{GHY} = \frac{\beta}{4G_N} \left(2r_\infty^2 - m - c \left(r_\infty^2 - \frac{m}{2} \right) + O\left(\frac{1}{r_\infty^2}\right) \right). \quad (3.55)$$

We can now add (3.44) and (3.55) to obtain

$$I_{EH} + I_{GHY} = \frac{\beta}{4G_N} \left(3r_\infty^2 - 2m - c \left(r_\infty^2 - \frac{m}{2} \right) + O\left(\frac{1}{r_\infty^2}\right) \right). \quad (3.56)$$

Finally, choosing $c = 3$ to cancel of divergent terms and taking $r_\infty \rightarrow \infty$, we find the final expression of the Euclidean action

$$I_E = \lim_{r_\infty \rightarrow \infty} (I_{EH} + I_{GHY}) = -\frac{\beta m}{8G_N}. \quad (3.57)$$

We can use this action in (3.40) and (3.41) to find an expression for the entropy of the spacetime. First, using

$$m = \frac{4\pi^2}{\beta^2} \quad (3.58)$$

we find the partition function to be

$$Z = e^{-I_E} = \exp\left(\frac{\pi^2}{2\beta G_N}\right) \quad (3.59)$$

and the entropy is given by

$$\begin{aligned} S &= (1 - \beta \partial_\beta) \log Z = \frac{\pi^2}{2\beta G_N} + \beta \left(\frac{\pi^2}{2\beta^2 G_N} \right) = \frac{\pi^2}{\beta G_N} \\ &\Rightarrow S = \frac{\pi \sqrt{m}}{2G_N} \end{aligned} \quad (3.60)$$

which is the same as the area-law calculation.

The utility of the semiclassical calculations comes from the fact that we do not need an event horizon to find the temperature and the entropy of the spacetime and will, in fact, be

necessary for the specific case of the $(3 + 1)$ -dimensional topological black hole due to the fact that the area-law calculations are unreliable since observers do not agree on the area of the event horizon.

3.5 Holographic Entanglement Entropy

Since the AdS/CFT conjecture relates all phenomena in the bulk and the CFT, we should expect there to be a bulk geometric dual to quantum entanglement entropy [2, 10]. The original proposal for the bulk calculation of the entanglement entropy, S_A , of a spatial region A was given by Ryu and Takayanagi and is given by

$$S_A = \frac{\text{Area}(\gamma)}{4G_N^{(d)}} \quad (3.61)$$

where γ is the minimal area surface terminating on the boundary of A and $G_N^{(d)}$ is Newton's gravitational constant for a d -dimensional spacetime [10]. This formulation of HEE relies on a calculation at a fixed time, so it is not naturally covariant. The covariant generalization was introduced by Hubeny-Rangamani-Takayanagi, but is not necessary for our particular calculation [11].

The motivation for the Ryu-Takayangi formula is as follows [30]: to find the entanglement entropy of a spatial subregion A of the total CFT on $\partial\mathcal{M}$, we must trace over all possible states of the CFT defined on the rest of the space \bar{A} . The act of tracing over all possible states on \bar{A} is admitting that an observation of the CFT on A does not give any information about the CFT on \bar{A} . To mirror this concept in the bulk, we should only consider observers which have access to the region A on the boundary. To do this, we must cut off the observer from the rest of the boundary by imposing an artificial horizon, given by the surface γ which ends on the boundary of A , ∂A (Figure 3.2). Since there is a continuous family of surfaces in the bulk which terminate on ∂A , to specify a unique surface, we choose the one with minimal area. However, we know that the entropy that this observer will see will be proportional to the area of γ due to the holographic entropy in the bulk theory.

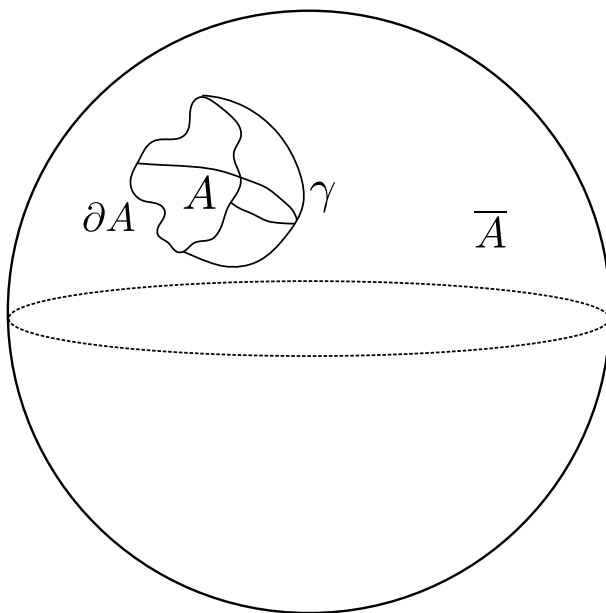


Figure 3.2: To calculate the entanglement entropy of the CFT on region A with the CFT on region \bar{A} , we calculate the area of the extremal-area surface, γ , which ends on the boundary of A , ∂A .

This formula is quite remarkable due to the fact that it allows us to find the entanglement entropy of a CFT, which is generally an incredibly difficult process, just by finding an area in the bulk spacetime, which is significantly simpler. Before we apply HEE to more complicated situations, it is worth checking the conjecture for situations for which we already know the answer, i.e. $(1 + 1)$ -dimensional CFTs for which we can use the Cardy formula.

3.5.1 $(1+1)$ -Dimensional CFT at Zero Temperature

As we have already stated, the $(d - 1)$ -dimensional CFT in its zero-temperature (i.e. vacuum) state is dual to global AdS_d . Using the simplest case of AdS_3 , we can define Poincaré coordinates (T, X, Z) in terms of the embedding coordinates (T_1, T_2, X_1, X_2)

$$\begin{aligned}
T_1 &= \frac{Z}{2} \left(1 + \frac{1}{Z^2} (1 + X^2 - T^2) \right) \\
T_2 &= \frac{T}{Z} \\
X_1 &= \frac{X}{Z} \\
X_2 &= \frac{Z}{2} \left(1 + \frac{1}{Z^2} (-1 + X^2 - T^2) \right)
\end{aligned} \tag{3.62}$$

which transform the metric (2.35) to

$$ds^2 = \frac{1}{Z^2} (-dT^2 + dX^2 + dZ^2) \tag{3.63}$$

with coordinate ranges $T \in (-\infty, \infty)$, $X \in (-\infty, \infty)$, and $Z \in (0, \infty)$ [22]. Since all of the embedding coordinates as well as the metric diverge at $Z = 0$, we associate this with the boundary of AdS_3 . A spatial region A of length $2R$ on the boundary is given by the range $X \in [-R, R]$ and $T = \text{const}$. Since the metric (3.63) is independent of T , which plays the role of time, a minimal area surface which terminates on the endpoints of A at any time will be valid at any other time, so for our calculation, we take $T = \text{const}$ in the bulk as well as the boundary. Therefore, our minimal area surface, γ , will be a spacelike line in the bulk which ends on $X = -R$ and $X = R$. We will parameterize this surface by Z so that $X = X(Z)$ on γ . The induced metric on this surface is given by

$$h = g_{\mu\nu} \frac{\partial x^\mu}{\partial Z} \frac{\partial x^\nu}{\partial Z} = \frac{1}{Z^2} \left(1 + \left(\frac{dX}{dZ} \right)^2 \right) \tag{3.64}$$

where x^μ are the coordinates on the full spacetime. The area of this surface is then given by

$$\text{Area}(\gamma) = \int dx \sqrt{h} = \int_a^b \frac{dZ}{Z} \sqrt{1 + \left(\frac{dX}{dZ} \right)^2} \tag{3.65}$$

and we will specify the bounds of the integral later. The integrand of (3.65) is a function of $X(Z)$, dX/dZ , and Z , so we can treat it as a Lagrangian

$$\mathcal{L} \left(X, \frac{dX}{dZ}; Z \right) = \frac{1}{Z} \sqrt{1 + \left(\frac{dX}{dZ} \right)^2} \tag{3.66}$$

which we can minimize with the standard Euler Lagrange equation [41]. Since the integrand of (3.65) does not explicitly depend on $X(Z)$, we can see that the Euler-Lagrange equation simplifies to

$$\frac{\partial \mathcal{L}}{\partial(dX/dZ)} = \frac{\frac{dX}{dZ}}{Z\sqrt{1 + \left(\frac{dX}{dZ}\right)^2}} = k \quad \Rightarrow \quad \frac{dX}{dZ} = \pm \frac{Z}{\sqrt{k^2 - Z^2}} \quad (3.67)$$

where k is an unknown constant. Integrating with respect to Z and using the boundary conditions, $X(0) = \pm R$, we find

$$X(Z) = \pm\sqrt{R^2 - Z^2}. \quad (3.68)$$

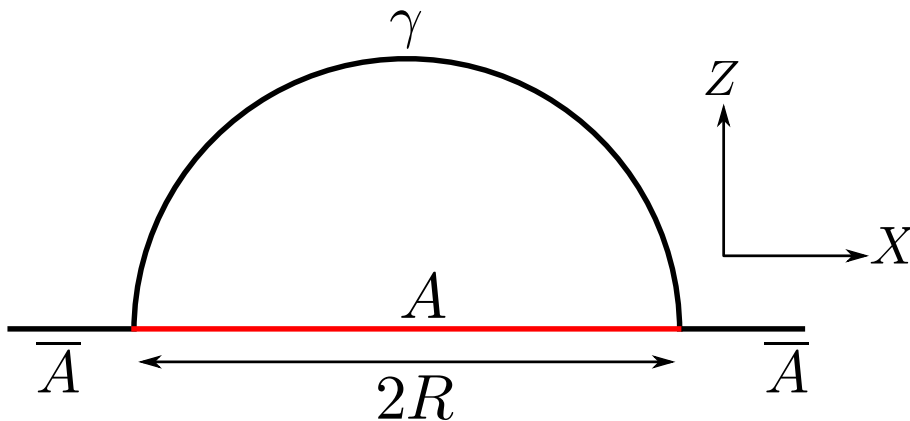


Figure 3.3: The entanglement entropy of the CFT on region A with length $2R$ can be calculated by the minimal area surface, γ , given by semicircles of radius R which intersect the boundary at right angles.

The extremal-area surface corresponding to region A on the boundary is just a circle which intersects the boundary at right angles (Figure 3.3). Since the maximum value that Z can take on this surface is R and the surface terminates at $Z = 0$, these are the upper and lower bounds on the integral, respectively. However, we will see that the area integral diverges from the region where $Z \rightarrow 0$, so we regularize by introducing a cutoff $0 < \epsilon \ll 1$ as the lower bound. Using this in (3.65) gives

$$\text{Area}(\gamma) = 2 \int_{\epsilon}^R dZ \frac{R}{Z} (R^2 - Z^2)^{-\frac{1}{2}} = 2 \log \left(\frac{2R}{\epsilon} \right) \quad (3.69)$$

for $R \gg \epsilon$. The multiplication by the factor of two comes from integration over a symmetric interval. From this, we can use HEE to say that the entanglement entropy of a spatial region A of a $(1+1)$ -dimensional CFT in its vacuum state is given by

$$S_A = \frac{1}{2G_N^{(3)}} \log \left(\frac{2R}{\epsilon} \right) \quad (3.70)$$

which agrees exactly with the result from the Cardy formula (3.11) if $c = 3 / \left(2G_N^{(3)} \right)$ (which is the central charge predicted by the AdS/CFT correspondence [42]). Though this spacetime is relatively simple, it shows that HEE can reproduce known results from direct calculations using CFTs.

3.5.2 (1+1)-Dimensional CFT at Finite Temperature

As shown by Maldacena, a $(1+1)$ -dimensional CFT at finite temperature $1/\beta$ is dual to the BTZ black hole which radiates at temperature $1/\beta$ [5]. Hence, a holographic approach using (3.61) should reproduce (3.12) for the BTZ spacetime. Beginning with metric (2.48), we can note that this spacetime is time-independent. We can then take $t = \text{const}$ and the extremal area surface, γ , will be a spacelike line which we will parameterize by r such that $\phi = \phi(r)$ on γ . The induced metric on γ is given by

$$h = g_{\mu\nu} \frac{\partial x^\mu}{\partial r} \frac{\partial x^\nu}{\partial r} = (r^2 - m)^{-1} + r^2 \left(\frac{d\phi}{dr} \right)^2 \quad (3.71)$$

and the area functional becomes

$$\text{Area}(\gamma) = \int dx \sqrt{h} = \int_a^b dr \sqrt{(r^2 - m)^{-1} + r^2 \left(\frac{d\phi}{dr} \right)^2}. \quad (3.72)$$

We can again find $\phi(r)$ by solving the Euler-Langrange equation

$$\frac{r^2 \frac{d\phi}{dr}}{\sqrt{(r^2 - m)^{-1} + r^2 \left(\frac{d\phi}{dr} \right)^2}} = k \quad \Rightarrow \quad \frac{d\phi}{dr} = \pm \sqrt{\frac{k^2}{r^2(r^2 - m)(r^2 - k^2)}}. \quad (3.73)$$

If we want the endpoints of region A to be at $\phi = \pm R$, we should expect a critical point at $r = r_*$ such that

$$\left(\frac{dr}{d\phi}\right)\Big|_{r=r_*} = 0 \quad \Rightarrow \quad \left(\frac{d\phi}{dr}\right)\Big|_{r=r_*} \rightarrow \infty \quad (3.74)$$

which is satisfied if $k = r_*$. If we assume $r_* > m$, from (3.73), we can see that this is the only critical value for $\phi(r)$ and so r_* corresponds to the minimum value of r (Figure 3.4). Since either R or r_* uniquely define the surface, we can relate them by integrating (3.73)

$$R = \int_{r_*}^{\infty} dr \sqrt{\frac{r_*^2}{r^2(r^2 - m)(r^2 - r_*^2)}} = \frac{1}{2\sqrt{m}} \log \left(\frac{r_* + \sqrt{m}}{r_* - \sqrt{m}} \right) \Rightarrow r_* = \sqrt{m} \coth(\sqrt{m} R). \quad (3.75)$$

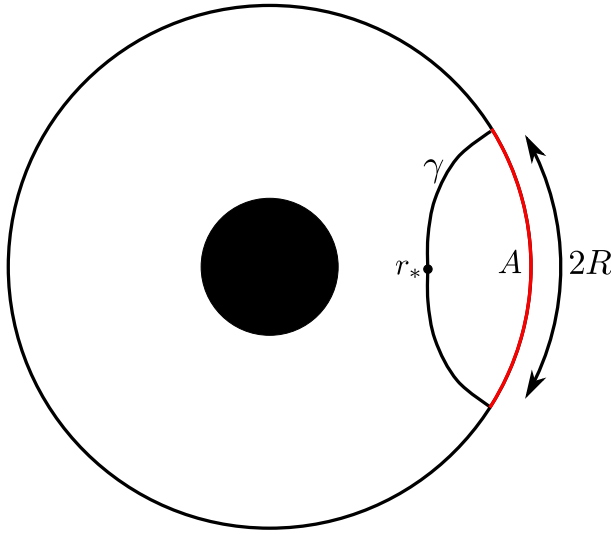


Figure 3.4: The minimal surface γ will have a critical point at $r = r_*$. Since γ is uniquely specified by either r_* or the length of the region A of the boundary, $2R$, we can use either to give γ .

Finally, we can use (3.73) in the area functional to find the area of the surface γ

$$\begin{aligned} \text{Area}(\gamma) &= 2 \int_{r_*}^{r_\infty} \frac{r dr}{\sqrt{(r^2 - m)(r^2 - r_*^2)}} = 2 \log(2r_\infty) - \log(r_*^2 - m) \\ &\quad \text{or} \\ \text{Area}(\gamma) &= 2 \log(2r_\infty) + \log \left(\frac{\sinh^2(\sqrt{m} R)}{m} \right) \end{aligned} \quad (3.76)$$

where r_∞ is a cutoff that we take to infinity. Using $r_\infty = 1/\epsilon$ with $0 < \epsilon \ll 1$, and the inverse temperature of the BTZ black hole (3.28), we find the entanglement entropy of a CFT on region A of length $2R$ is given by

$$S_A = \frac{1}{2G_N^{(3)}} \log \left(\frac{\beta}{\pi\epsilon} \sinh \frac{2\pi R}{\beta} \right) \quad (3.77)$$

which agrees with (3.12).

An easier way to arrive at the result (3.77) is to recall that the BTZ solution is locally AdS and so we can relate BTZ coordinates to Poincaré coordinates [11]. We first define null Poincaré coordinates

$$W_\pm = X \pm T \quad (3.78)$$

so that the metric (3.63) becomes [11, 22]

$$ds^2 = \frac{1}{Z^2} (dW_+ dW_- + dZ^2). \quad (3.79)$$

The coordinates of the BTZ black hole are related to null Poincaré coordinates by [46]

$$\begin{aligned} W_\pm &= \sqrt{\frac{r^2 - m}{r^2}} e^{\sqrt{m}(\phi \pm t)} \\ Z &= \frac{\sqrt{m}}{r} e^{\sqrt{m}\phi}. \end{aligned} \quad (3.80)$$

If our surface is anchored to the boundary at time $t = t_0$ with endpoints ϕ_1 and ϕ_2 , we can represent the cutoff in Poincaré coordinates in terms of r_∞

$$\epsilon_{1,2} = \frac{\sqrt{m}}{r_\infty} e^{\sqrt{m}\phi_{1,2}} \quad (3.81)$$

and a region of the boundary ΔX is given by

$$\begin{aligned} (\Delta X)^2 &= \Delta W_+ \Delta W_- = \left(e^{\sqrt{m}(\phi_2 + t_0)} - e^{\sqrt{m}(\phi_1 + t_0)} \right) \left(e^{\sqrt{m}(\phi_2 - t_0)} - e^{\sqrt{m}(\phi_1 - t_0)} \right) \\ &\Rightarrow (\Delta X)^2 = \left(e^{\sqrt{m}\phi_2} - e^{\sqrt{m}\phi_1} \right)^2. \end{aligned} \quad (3.82)$$

Using these values in (3.69)

$$\text{Area}(\gamma) = \log\left(\frac{(\Delta X)^2}{\epsilon_1 \epsilon_2}\right) = 2\log(2r_\infty) + \log\left(\frac{\sinh^2(\sqrt{m}R)}{m}\right) \quad (3.83)$$

we recover the area of γ for the BTZ spacetime after defining $R = (\phi_2 - \phi_1)/2$.

One interesting aspect of HEE for the BTZ black hole is that it actually predicts that the boundary CFT as a whole should be in a mixed state [10, 16, 30]. To see this, we recognize that the event horizon, $r = \sqrt{m}$, is also a valid solution to the Euler-Lagrange equations which minimize (3.72). However, this surface does not terminate on the boundary, so for it to be included in the holographic entanglement entropy, we must combine it with the surface γ , i.e. take $\gamma \cup H$ where H is the event horizon. Since the surface γ is spacelike, it will minimize the area, so the combined area of $\gamma \cup H$ will never be less than that of γ . However, as R increases, (3.76) also increases, so we expect there to be some value of R such that $\text{Area}(\gamma' \cup H) < \text{Area}(\gamma)$ where $\text{Area}(\gamma' \cup H)$ is given by

$$\text{Area}(\gamma' \cup H) = 2\log(2r_\infty) + \log\left(\frac{\sinh^2(\sqrt{m}(\pi - R))}{m}\right) + 2\pi\sqrt{m} \quad (3.84)$$

where γ' is the same surface as γ , but with $R \rightarrow \pi - R$. We find that $\text{Area}(\gamma' \cup H) < \text{Area}(\gamma)$ for $R < \pi$, so (3.84) is the valid area calculation for $R \rightarrow \pi$, which corresponds to region A becoming the full boundary (Figure 3.5) [10, 16, 30]. In the limit as $R = \pi$ and $r_\infty \rightarrow \infty$, the logarithmic terms cancel and we are only left with the area of the event horizon and so the entanglement entropy of the full boundary CFT is given by

$$S_{\text{CFT}} = \frac{\pi\sqrt{m}}{2G_N^{(3)}} \quad (3.85)$$

which is exactly the entropy of the black hole.

Since the CFT is in a mixed state, we can attempt to find a purification, which will be the copy of the CFT on this boundary and the other copy of the CFT on the second boundary from the maximal extension, as we will see in the next section.

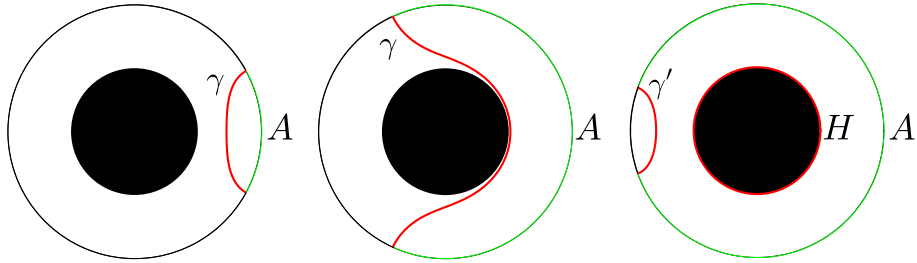


Figure 3.5: Minimal area surface, γ (red), corresponding to different sizes of region A (green) on the boundary. When A reaches a certain size, $\gamma' \cup H < \gamma$ becomes the minimal area surface, and when A is the full boundary, only the area of the event horizon remains.

3.5.3 BTZ Boundary Theory

To find the purification of the CFT dual to the BTZ black hole, we begin by defining global coordinates for AdS_3

$$\begin{aligned}
 T_1 &= \frac{1+r^2}{1-r^2} \cos t \\
 T_2 &= \frac{1+r^2}{1-r^2} \sin t \\
 X_1 &= \frac{2r}{1-r^2} \cos \theta \\
 X_2 &= \frac{2r}{1-r^2} \sin \theta
 \end{aligned} \tag{3.86}$$

with $r \in [0, 1)$, $t, \theta \in (0, 2\pi]$ [23]. As in section 2.5, to avoid closed timelike curves, we adopt a universal covering where $t \in (-\infty, \infty)$. The metric becomes

$$ds^2 = \frac{4}{(1-r^2)^2} \left(-\frac{1}{4} (1+r^2)^2 dt^2 + dr^2 + r^2 d\theta \right). \tag{3.87}$$

The Killing vector which generates the quotient will be given by $\xi = -X_1 \partial_{T_1} - T_1 \partial_{X_1}$ and we can identify an orthogonal Killing vector given by $\eta = X_2 \partial_{T_2} + T_2 \partial_{X_2}$ [38, 39]. We can transform (3.87) by a conformal factor, $\Omega^2 = (1-r^2)^2/4$ and take $r \rightarrow 1$ to obtain the metric on the conformal boundary

$$d\sigma^2 = -dt^2 + d\theta^2. \tag{3.88}$$

The conformal Killing vectors generated by ξ and η on the boundary are given by [39]

$$\begin{aligned}
\xi_b &= \sin t \cos \theta \partial_t + \cos t \sin \theta \partial_\theta \\
\eta_b &= \cos t \sin \theta \partial_t + \sin t \cos \theta \partial_\theta.
\end{aligned}
\tag{3.89}$$

Since ξ_b will generate the quotient in the boundary theory, we will only keep the regions where $\xi_b^2 > 0$ to avoid closed timelike curves. These are given by the two disconnected diamonds [38, 39]

$$\begin{aligned}
D_R &= \left\{ (t, \theta) \left| 0 < \theta < \pi, |t| < \frac{\pi}{2} - \left| \theta - \frac{\pi}{2} \right| \right. \right\} \\
D_L &= \left\{ (t, \theta) \left| -\pi < \theta < 0, |t| < \frac{\pi}{2} - \left| \theta + \frac{\pi}{2} \right| \right. \right\}.
\end{aligned}
\tag{3.90}$$

The regions D_R and D_L correspond to the two separate asymptotic boundaries that result from quotienting AdS_3 to obtain the BTZ black hole. We also note that η_b is timelike in both regions, but points in the future timelike direction in region D_R and the past timelike direction in region D_L . Since η is timelike, when defining particle excitations in the boundary theory, we associate positive energy modes with the region where η points to the future, while we define negative energy modes in the region where η points to the past [18, 36] (Figure 3.6). Therefore, the total Hilbert space will be given by $\mathcal{H} = \mathcal{H}_R \otimes \mathcal{H}_L$ and we can describe the total state by a thermofield double

$$|\Psi\rangle = \frac{1}{\sqrt{Z(\beta)}} \sum_n e^{-\beta E_n/2} |E_n\rangle_R \otimes |E_n\rangle_L
\tag{3.91}$$

which suggests particles in D_R are entangled with particles in D_L [5, 17].

The case of the BTZ black hole has given us insight into the dual CFT of black holes. We have seen that the CFT shares the thermal properties of the black hole, and that the entropy of the total CFT is the entropy of the black hole. Since the CFT is in a mixed state, we naturally purify it with a CFT on the second copy of the boundary from the maximal extension.

However, this seems to force the (3+1)-dimensional topological black hole into a paradox. If the black hole is thermal, we would expect the CFT to also be thermal. But if the CFT

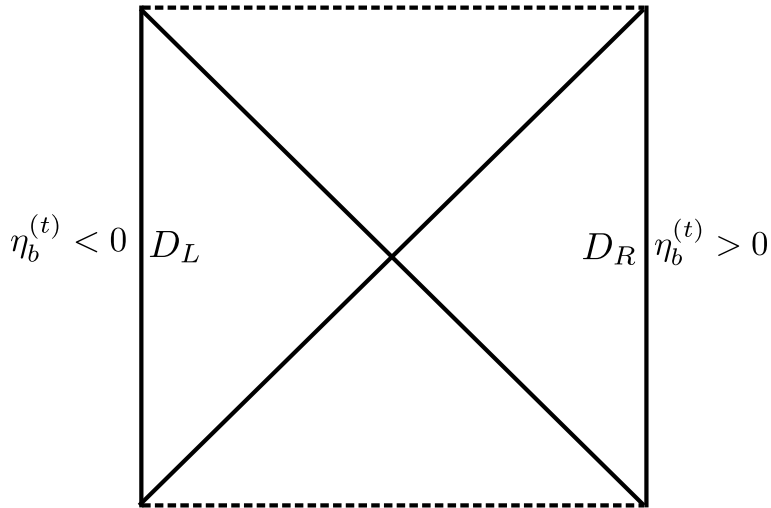


Figure 3.6: Penrose diagram of the maximally extended BTZ black hole. Here, there are two distinct boundaries, D_R and D_L , on which η_b is a timelike Killing vector. On D_R , the t -component of η_b ($\eta_b^{(t)}$) is positive, and so we associate this region with positive energy modes, while on D_L , $\eta_b^{(t)}$ is negative, so we associate this region with negative energy modes.

is thermal, it can typically be interpreted as being in a mixed state and we should be able to find a suitable purification. However, recall that this black hole only has a single boundary so the possible purification is unclear. This contradiction is what motivates us to study the $(3+1)$ -dimensional topological black hole as an interesting test of the holographic entanglement entropy conjecture.

3.5.4 Strip on Boundary of AdS_d

The final known result we give is a generalization of the results of section 3.5.1 to AdS_d for $d > 3$. The region A on the boundary will be given by a strip with width R and “length” L^{d-3} (Figure 3.7). In this calculation, we assume that L is held constant and we can vary R . The metric for AdS_d in Poincaré coordinates is given by

$$ds^2 = \frac{1}{Z^2} \left(-dT^2 + dX^2 + \sum_{i=1}^{d-3} dY_i^2 + dZ^2 \right) \quad (3.92)$$

where $\{T, X, Y_i\} \in (-\infty, \infty)$ and $Z \in (0, \infty)$ [22]. The region A on the boundary at $Z = 0$ will be given by $X \in [-R/2, R/2]$, $Y_i \in [-L/2, L/2]$. Since we are fixing L and varying R we

can parametrize the surface, γ , by Z so that $X = X(Z)$. The area of γ is therefore [11, 30]

$$\text{Area}(\gamma) = \prod_{i=1}^{d-3} \int_{-L/2}^{L/2} dY_i \int_a^b \frac{dZ}{Z^{d-2}} \sqrt{1 + \left(\frac{dX}{dZ}\right)^2}. \quad (3.93)$$

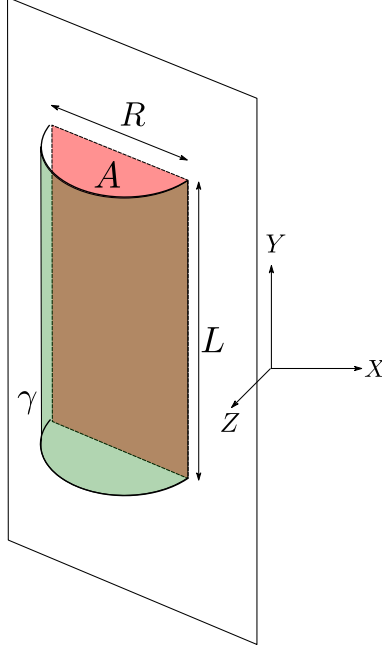


Figure 3.7: Minimal area surface, γ (green) corresponding to strip A of the boundary (red). The strip has length L and width R .

The Euler-Lagrange equation yields

$$\frac{dX}{dZ} = \frac{Z^{d-2}}{\sqrt{Z_*^{2(d-2)} - Z^{2(d-2)}}} \quad (3.94)$$

where Z_* is the turning point of γ (analogous to r_* in the BTZ example). We can relate Z_* to R by integrating

$$\frac{R}{2} = \int_0^{Z_*} dZ \frac{Z^{d-2}}{\sqrt{Z_*^{2(d-2)} - Z^{2(d-2)}}} = \frac{\sqrt{\pi} \Gamma\left(\frac{d-1}{2(d-2)}\right)}{\Gamma\left(\frac{1}{2(d-2)}\right)} Z_*. \quad (3.95)$$

The area of the γ is then given by [11, 30]

$$\begin{aligned}
\text{Area}(\gamma) &= 2L^{d-3} \int_{\epsilon}^{Z_*} dZ \frac{Z_*^{d-2}}{Z^{d-2}} (Z_*^{2(d-2)} - Z^{2(d-2)})^{-\frac{1}{2}} \\
\Rightarrow \text{Area}(\gamma) &= \frac{2}{d-3} \left(\frac{L}{\epsilon}\right)^{d-3} - \frac{2^{d-2} \pi^{(d-2)/2}}{d-3} \left(\frac{\Gamma\left(\frac{d-1}{2(d-2)}\right)}{\Gamma\left(\frac{1}{2(d-2)}\right)}\right)^{d-2} \left(\frac{L}{R}\right)^{d-3}. \quad (3.96)
\end{aligned}$$

The entanglement entropy of region A will then be given by this area divided by $4G_N^{(d)}$. This result will play a crucial role in our analysis of the $(3+1)$ -dimensional topological black hole.

CHAPTER 4
TIME-DEPENDENT BLACK HOLES IN HOLOGRAPHIC ENTANGLEMENT
ENTROPY

Up to this point, we have discussed known results to build the machinery to analyze the $(3 + 1)$ -dimensional topological black hole. This chapter will be dedicated to this specific spacetime and its behavior in terms of the holographic entanglement entropy. We begin the discussion by explicitly calculating the area of the event horizon according to different observers in section 4.1 to further motivate interest in this particular spacetime. In section 4.2, we go through the holographic calculation of entanglement entropy. In section 4.3, we go through a deeper analysis of the thermodynamic properties of the black hole. Finally, in section 4.4, we find the regions in the boundary CFT which support particles and compare these results to those in section 4.2.

4.1 Observer-Dependent Event Horizon

As we have seen, the thermodynamics of a black hole are deeply tied to the area of the event horizon. In polar Kruskal coordinates, (2.58), at a constant time-slice, $t = t_0$, the event horizon is located at $\chi = t_0$. The induced metric on the horizon is then given by

$$d\sigma_{\chi=t_0}^2 = 4t_0^2 d\theta^2 + d\phi^2. \quad (4.1)$$

and the square root of the determinate of the induced metric is

$$\sqrt{h} = 2|t_0|. \quad (4.2)$$

The area of the event horizon is then given by

$$\text{Area}(\chi = t_0) = 2|t_0| \int_0^{2\pi} d\theta \int_0^{2\pi} d\phi = 8\pi^2 |t_0|. \quad (4.3)$$

which exhibits a time-dependence.

If we instead examine the spacetime in full exterior coordinates (2.60) or static coordinates

(2.63), where the event horizon is located at $\rho = 0$, we find the induced metric to be

$$d\sigma_{\rho=0} = d\phi^2 \tag{4.4}$$

which is simply the metric of the unit circle. Since this is a 1-dimensional surface, it necessarily has zero area in a $(3 + 1)$ -dimensional spacetime.

This poses an issue that the holographic entanglement entropy must overcome. As we have seen, the entanglement entropy of the total CFT is closely related to the area of event horizons in the bulk. However, if observers cannot agree on the area of the horizon, we may expect different results from the holographic calculation. A natural resolution would be if the observers in question see different boundary regions, analogous to the inertial versus accelerated observers in AdS [17, 31]. However, since these observers both have access to the full boundary, they should both be suitable candidates for the geometric dual to the full CFT. Therefore, if the region, A , of the boundary does not change between coordinate systems, the entanglement entropy of the region should not change either. Hence, this seemingly creates a paradox which we must overcome to verify the holographic entanglement entropy conjecture.

4.2 Holographic Calculation

To compute the area of the extremal area surface, γ , which terminates on the boundary of A , we will use the method introduced in section 3.5.2 of realizing the topological black hole as locally AdS_4 and relating it to the area corresponding to a strip on the boundary with length L and width R , given by (3.96)

$$\text{Area}(\gamma_P) = 2 \left(\frac{L}{\epsilon} \right) - \alpha \left(\frac{L}{R} \right) \tag{4.5}$$

where γ_P is the minimal area surface in AdS_4 and

$$\alpha = 4\pi \left(\frac{\Gamma\left(\frac{3}{4}\right)}{\Gamma\left(\frac{1}{4}\right)} \right)^2 \tag{4.6}$$

is a constant. We first apply HEE for the case of Kruskal coordinates. Polar Kruskal coordinates (2.58), are related to null Poincaré coordinates by

$$\begin{aligned}
W_{\pm} &= X \pm T = \frac{2}{1 - t^2 + \chi^2} (\chi \cos \theta \pm t) e^{\phi} \\
Y &= \frac{2}{1 - t^2 + \chi^2} \chi \sin \theta e^{\phi} \\
Z &= \frac{1 + t^2 - \chi^2}{1 - t^2 + \chi^2} e^{\phi}
\end{aligned} \tag{4.7}$$

In these coordinates, the boundary is the surface where $Z \rightarrow 0$, which corresponds to $\chi = \sqrt{1 + t^2}$. If we anchor the surface γ to the boundary at fixed time $t = t_0$ such that $\theta \in [\theta_1, \theta_2]$ and $\phi \in [\phi_1, \phi_2]$, the cutoff at $Z = \epsilon \ll 1$ corresponds to

$$\epsilon_{1,2} = a e^{\phi_{1,2}} \quad \text{where} \quad 0 < a \ll 1. \tag{4.8}$$

For convenience, we center A so that $\theta_1 = -\Theta$ and $\theta_2 = \Theta$ and the length, L , of A is given by

$$L = \Delta Y = \sqrt{1 + t_0^2} (e^{\phi_2} + e^{\phi_1}) \sin \Theta \tag{4.9}$$

and the width, R is given by

$$R^2 = \Delta W_+ \Delta W_- = (e^{\phi_2} - e^{\phi_1})^2 [(1 + t_0^2) \cos^2 \Theta - t_0^2]. \tag{4.10}$$

Using (4.8), (4.9), and (4.10) in (4.5), we find an expression for the area using $\epsilon^2 = \epsilon_1 \epsilon_2$

$$\text{Area}(\gamma) = 4 \left(\frac{\cosh \Delta}{a} \right) \sin \Theta - \alpha \left(\frac{\sqrt{1 + t_0^2} \sin \Theta}{\sqrt{(1 + t_0^2) \cos^2 \Theta - t_0^2}} \right) \coth \Delta \tag{4.11}$$

where $\Delta = (\phi_2 - \phi_1)/2$. From this expression, we can see that the surface γ is restricted to the region

$$(1 + t_0^2) \cos^2 \Theta - t_0^2 > 0. \tag{4.12}$$

Similarly, we can perform the same HEE calculation with full exterior coordinates, which are related to null Poincaré coordinates by

$$\begin{aligned}
W_{\pm} &= \frac{2\rho}{1+\rho^2} (\cosh \tau \cos \theta \pm \sinh \tau) e^{\phi} \\
Y &= \frac{2\rho}{1+\rho^2} \cosh \tau \sin \theta e^{\phi} \\
Z &= \frac{1-\rho^2}{1+\rho^2} e^{\phi}.
\end{aligned} \tag{4.13}$$

For fixed time on the boundary $\tau = \tau_0$ and endpoints $(-\Theta, \phi_1)$ and (Θ, ϕ_2) , we find that the cutoff is given by

$$\epsilon_{1,2} = a e^{\phi_{1,2}}, \tag{4.14}$$

the length of region A is given by

$$L = \cosh \tau_0 (e^{\phi_2} + e^{\phi_1}) \sin \Theta \tag{4.15}$$

and the width

$$R^2 = (e^{\phi_2} - e^{\phi_1})^2 (\cosh^2 \tau_0 \cos^2 \Theta - \sinh^2 \tau_0). \tag{4.16}$$

Using these values in (4.5) gives the area of the surface γ in full exterior coordinates

$$\text{Area}(\gamma) = 4 \left(\frac{\cosh \Delta}{a} \right) \sin \Theta - \alpha \left(\frac{\cosh \tau_0 \sin \Theta}{\sqrt{\cosh^2 \tau_0 \cos^2 \Theta - \sinh^2 \tau_0}} \right) \coth \Delta. \tag{4.17}$$

If we examine the coordinates (2.57) and (2.60), we can see that $\cosh \tau_0 = \sqrt{1+t_0^2}$, and so (4.11) and (4.17) are the same expression. In these coordinates, the surface is restricted to

$$\cosh^2 \tau_0 \cos^2 \Theta - \sinh^2 \tau_0 > 0 \tag{4.18}$$

on the boundary.

We recall that static coordinates (2.63) are confined to

$$y_1^2 - t^2 > 0 \Rightarrow \chi^2 \cos^2 \theta - t^2 > 0 \tag{4.19}$$

which on the boundary, $t = t_0$, $\chi = \sqrt{1+t_0^2}$ (or $\rho = \cosh \tau_0$), $\theta = \Theta$, corresponds to exactly (4.12) and (4.18). Therefore, it seems static coordinates are naturally adapted to the HEE calculation.

We also note that, as $(1 + t_0^2) \cos^2 \Theta - t_0^2 \rightarrow 0$ ($\cosh^2 \tau_0 \cos^2 \Theta - \sinh^2 \tau_0 \rightarrow 0$) and $a \rightarrow 0$, i.e. we take the region A to be the full boundary of static coordinates, the area of γ also goes to zero. This suggests that the CFT on the full boundary in static coordinates is in a pure state.

As we should expect, the entanglement entropy of the CFT on region A of the boundary does not vary between coordinate systems using the holographic calculation. However, we have arrived at the somewhat surprising result that there is a preferred coordinate system for the HEE calculation: the static coordinates.

4.3 Thermodynamics of the Topological Black Hole

In section 4.1, we found that the area of the event horizon gave an inconsistent measure of the entropy of the spacetime, and so we will resort to the semiclassical calculation instead. In this section, we wish to discuss the thermodynamics of the bulk, but only in the portion of the spacetime for which γ is well defined. Therefore, we will restrict our attention to static coordinates. Taking $\tau \rightarrow -i\tau_E$ in (2.63), the metric becomes

$$ds^2 = \frac{4}{(1 - \rho^2)^2} [\rho^2 \sin^2 \theta d\tau_E^2 + d\rho^2 + \rho^2 d\theta^2] + \left(\frac{1 + \rho^2}{1 - \rho^2} \right)^2 d\phi^2. \quad (4.20)$$

The term in the square brackets is the metric of the 3-ball if τ_E is periodic with periodicity $\tau_E = \tau_E + 2\pi$. The inverse temperature of the spacetime is equal to the periodicity of the imaginary time component and so the spacetime has temperature

$$T = \frac{1}{2\pi}. \quad (4.21)$$

We notice that, unlike the BTZ black hole in section 3.4.2, we did not need to take a near horizon limit to find the temperature of the spacetime. We therefore conclude that the entire space is thermal, not just the black hole. This should be expected, since we can obtain the $(3+1)$ -dimensional topological black hole from a double Wick rotation of thermal AdS_4 [14].

Since β does not depend on the physical parameters of the space, as it did in section 3.4.2, from the form of (3.42) and (3.45), we can see that $I_E \propto \beta$. Using (3.40) and (3.41),

we can see that if the Euclidean action is linear in β , the entropy will be zero. This agrees with the result that the entire CFT defined on this region is in a pure state. Now, we can analyze the theory on the boundary to give a possible candidate for the CFT dual to the topological black hole.

4.4 Restriction of Particle Modes on Boundary

To examine the theory on the boundary, we will follow a similar approach as in section 3.5.3. First, we define global coordinates on AdS₄

$$\begin{aligned} T_1 &= \frac{1+r^2}{1-r^2} \cos t \quad , \quad T_2 = \frac{1+r^2}{1-r^2} \sin t \\ X_1 &= \frac{2r}{1-r^2} \cos \lambda \quad , \quad X_2 = \frac{2r}{1-r^2} \cos \theta \sin \lambda \quad , \quad X_3 = \frac{2r}{1-r^2} \sin \theta \sin \lambda \end{aligned} \quad (4.22)$$

with ranges $r \in [0, 1)$, $\theta \in (0, 2\pi]$, $\lambda \in [0, \pi]$ and $t \in (-\infty, \infty)$ after enforcing a universal covering to avoid closed timelike curves [23]. The metric (2.55) becomes

$$ds^2 = \frac{4}{(1-r^2)^2} \left(-\frac{(1+r^2)^2}{4} dt^2 + dr^2 + r^2 d\lambda^2 + r^2 \cos^2 \lambda d\theta^2 \right) \quad (4.23)$$

where the boundary is located at $r = 1$. The Killing vector that generates the quotient is given by $\xi = -X_1 \partial_{T_1} - T_1 \partial_{X_1}$ and we can see that the Killing vector $\eta = X_2 \partial_{T_2} + T_2 \partial_{X_2}$ is orthogonal to ξ . To get the metric on the boundary, we multiply (4.23) by the conformal factor $\Omega^2 = (1-r^2)^2/4$ and take $r \rightarrow 1$ to obtain

$$d\sigma^2 = -dt^2 + d\lambda^2 + \cos^2 \lambda d\theta^2. \quad (4.24)$$

The conformal Killing vectors on the boundary corresponding to ξ and η are given by

$$\begin{aligned} \xi_b &= \cos \lambda \sin t \partial_t + \cos t \sin \lambda \partial_\lambda \\ \eta_b &= \cos t \sin \lambda \cos \theta \partial_t + \sin t \cos \lambda \cos \theta \partial_\lambda - \sin t \csc \lambda \sin \theta \partial_\theta \end{aligned} \quad (4.25)$$

respectively. To find the region on the boundary that will survive the quotient, we find the region where $\xi_b^2 > 0$. Due to the range of λ , this only gives a single diamond

$$\left\{ (\lambda, t) \mid 0 < \lambda < \pi, |t| < \frac{\pi}{2} - \left| \lambda - \frac{\pi}{2} \right| \right\}. \quad (4.26)$$

This is in contrast to the BTZ black hole, which returned two distinct diamonds on the boundary and is a reflection of the fact that the $(3 + 1)$ -dimensional topological black hole only has a single, connected boundary. To better understand the action of ξ_b on the boundary space, we define the coordinates (inspired by those used in [38])

$$\begin{aligned} \alpha &= -\log \left[\tan \left(\frac{\lambda - t}{2} \right) \right] \\ \beta &= \log \left[\tan \left(\frac{\lambda + t}{2} \right) \right] \end{aligned} \quad (4.27)$$

giving the metric

$$d\sigma^2 = \frac{1}{\cosh \alpha \cosh \beta} \left(d\alpha d\beta + \cosh^2 \left(\frac{\alpha + \beta}{2} \right) d\theta^2 \right) \quad (4.28)$$

where the conformal Killing vectors are now given by

$$\begin{aligned} \xi_b &= -\partial_\alpha + \partial_\beta \\ \eta_b &= \cos \theta (\partial_\alpha + \partial_\beta) - \sin \theta \tanh \left(\frac{\alpha + \beta}{2} \right) \partial_\theta. \end{aligned} \quad (4.29)$$

The vector ξ_b maps the point $(\alpha, \beta, \theta) \rightarrow (\alpha - a, \beta + a, \theta)$. Unfortunately, the metric (4.28) is not invariant under an action generated by ξ_b , but the conformally equivalent metric

$$d\sigma^2 = d\alpha d\beta + \cosh^2 \left(\frac{\alpha + \beta}{2} \right) d\theta^2 \quad (4.30)$$

is. Finally, defining $\alpha = \tau - \phi$ and $\beta = \tau + \phi$, where $\{\tau, \phi\} \in (-\infty, \infty)$, we obtain the metric

$$ds^2 = -d\tau^2 + \cosh^2 \tau d\theta^2 + d\phi^2 \quad (4.31)$$

and the conformal Killing vectors take the form

$$\begin{aligned}\xi_b &= \partial_\phi \\ \eta_b &= \cos\theta \partial_\tau - \sin\theta \tanh\tau \partial_\theta.\end{aligned}\tag{4.32}$$

A quotient by ξ_b makes the identification $\phi = \phi + 2\pi n$ for $n \in \mathbb{Z}$ and we see that the metric (4.30) is the conformal boundary of the topological black hole in full exterior coordinates (2.60).

Near $\tau = 0$, we find $\eta_b = \cos\theta \partial_\tau$ is purely timelike, except for the points $\theta = \pi/2$ and $\theta = -\pi/2$. Moreover, for $-\pi/2 < \theta < \pi/2$, η_b points in the future direction, while for $\pi/2 < \theta < 3\pi/2$, η_b points in the past direction. Therefore, we naturally associate η_b with particle modes in the boundary theory, where positive energy modes are associated with the region where η_b is future-directed, while negative energy modes are associated with the region where η_b is past-directed [18, 36].

As the system evolves away from $\tau = 0$, we find that η_b is no longer timelike on the whole boundary. Since we associate particle modes with time, the particles are not well defined on the regions where η_b is spacelike and so the particles will be restricted to the regions given by [18, 36]

$$\eta_b^2 = -\cos^2\theta + \sin^2\theta \sinh^2\tau < 0.\tag{4.33}$$

Using standard trigonometric and hyperbolic trigonometric identities, we find that this is equivalent to the regions which satisfy

$$\cosh^2\tau \cos^2\theta - \sinh^2\tau > 0\tag{4.34}$$

but this is exactly the region of the boundary which the surface γ is restricted to (4.18). This is result that could have been anticipated, since we would not expect to have contributions to entanglement entropy from regions of the CFT on which we cannot have particles.

The fact that the area of the surface γ goes to zero as the region A encompasses one entire part of the boundary on which particles are allowed suggests that each of the two

particle-supporting regions are in a pure state. This is verified by the fact that the portion of the spacetime corresponding to each region has zero entropy. However, the spacetime also has a non-zero temperature, suggesting that the dual CFT is still thermal. Therefore, we conclude that the dual CFT is split into two regions, each in a pure, thermally populated state. This is in contrast to the case of the BTZ black hole, where we had two distinct CFTs, each in a mixed, thermally populated state. Figure 4.1 gives a pictorial representation of these findings, which can be contrasted to Figure 3.6.

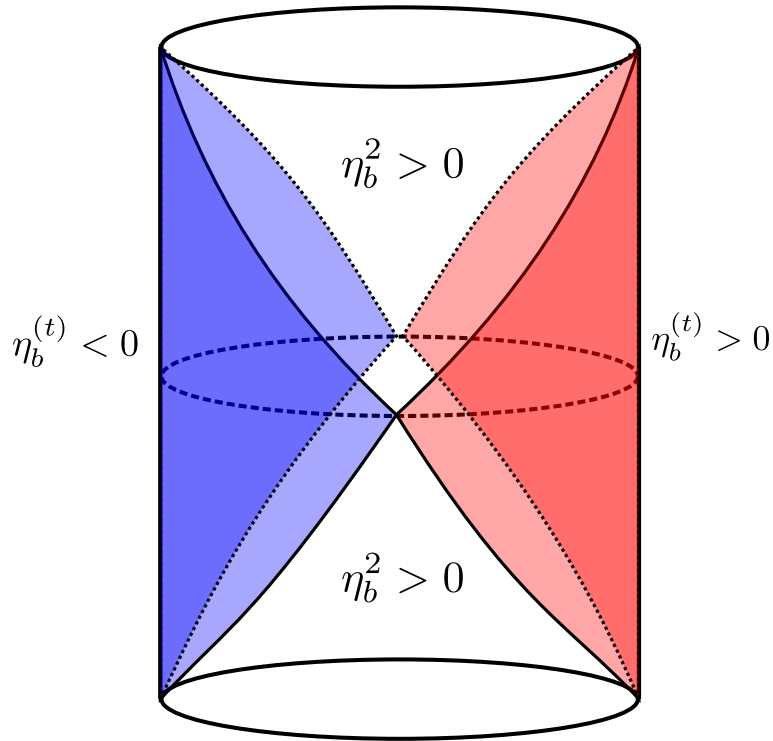


Figure 4.1: Diagram of the boundary of the topological black hole. The dashed circle represents $t = \tau = 0$, where η_b is timelike over the whole boundary. We see two distinct regions on the boundary where η_b is timelike, one where the time component, $\eta_b^{(t)}$, is positive, which we associate with positive energy modes (red), while on the other, $\eta_b^{(t)}$ is negative, which we associate with negative energy modes (blue). This figure is in contrast to Figure 3.6 since the latter shows two distinct boundaries where the modes are defined, while this shows two regions of the same boundary where modes are defined.

CHAPTER 5

CONCLUSIONS AND OUTLOOK

In condensed matter systems and general quantum field theories, it is important to know the number of degrees of freedom which contribute to the dynamical behavior of the system. One way of counting these degrees of freedom is by calculating the entanglement entropy of the system in question. However, analytical results for entanglement entropy directly from quantum field theory rarely stray from the well understood 2-dimensional systems due to the complicated calculations involved.

Holographic entanglement entropy attempts to solve these issues by proposing that entanglement entropy in a CFT can be calculated from areas in the dual spacetime. Up to this point, most holographic calculations have been restricted to the relatively simple settings of spacetimes in $(2 + 1)$ -dimensions and CFTs in $(1 + 1)$ -dimensions which exhibit no time-dependence. To use HEE for physical systems, the results of the results in $(2+1)$ -dimensional spacetimes and $(1+1)$ -dimensional CFTs must be generalized to higher dimensions and time-dependent systems. We hope to further this goal through our work.

The case of the $(3+1)$ -dimensional topological black hole is of interest due to the fact that it is a time-dependent spacetime with an observer-dependent event horizon. While horizons which vary between observers appear elsewhere in relativity, this particular case allows two observers with access to the full boundary to see different event horizon areas. In previous holographic entanglement entropy calculations, it has been shown that entanglement of the CFT on the boundary is closely related to the area of event horizons in the bulk. This suggests the possibility of an observer-dependence in holographic entanglement entropy.

While our calculation of HEE shows no observer-dependence, it does suggest that there is a preferred coordinate system for the calculation, i.e. static coordinates, which is somewhat surprising given that the coordinates do not cover the full space. Moreover, these coordi-

nates are such that the metric is time-independent, i.e. has a global timelike Killing vector. Since the region of the space which these coordinates cover correspond exactly to the region in the boundary theory where the Killing vector associated with particle modes is timelike, we expect this to hold for other spacetimes as well. This is a powerful result, since the time-independent holographic entanglement entropy calculation of Ryu-Takayanagi is significantly less involved than the covariant prescription of Hubeny-Rangamani-Takayanagi. This result also shows that, while holographic entanglement entropy can give insight to the properties of the dual CFT, it can also predict the regions in the CFT where particles are disallowed.

There is further work to be done by generalizing these results to other time-dependent spacetimes and their corresponding CFT duals, as well as generalizing these results to higher dimensions. This would ensure that the findings in this thesis hold for all cases outside of the particular one we studied.

We conclude by noting that the AdS/CFT correspondence is still only conjectured and so there is still much work to be done. Works such as this thesis serve to test the theory's consistency and help to verify it as the most promising theory of quantum gravity to date.

REFERENCES CITED

- [1] J.L. Cardy, “Is there a c theorem in four-dimensions?,” *Phys. Lett* **B215** (1988) 749-752.
- [2] J. Maldacena, “The large N limit of superconformal field theories and supergravity,” *Adv. Theor. Math. Phys* **2** (1998) 231-252.
- [3] C. Frances, “The conformal boundary of anti-de Sitter space-times,” *AdS/CFT correspondence: Einstein metrics and their conformal boundaries, Lect. Math. Theor. Phys.* **8** 205-216.
- [4] M. Schottenloher, *A Mathematical Introduction to Conformal Field Theory*. Berlin, DE: Springer-Verlag, 1997.
- [5] J.M. Maldacena, “Eternal Black Holes in AdS,” *JHEP* **0304** (2003) 021.
- [6] J.M. Bardeen, B. Carter, S.W. Hawking, “The four laws of black hole mechanics,” *Commun. mat. Phys* **31** (1973) 161-170.
- [7] S.W. Hawking, “Black holes in general relativity,” *Commun. math. Phys.* **25** (1972) 152-166.
- [8] S.W. Hawking, “Particle creation by black holes,” *Commun. math. Phys* **43** (1975) 199-220.
- [9] J. D. Bekenstein, “Black holes and entropy,” *Phys. Rev. D* **Vol. 7, Num. 8** (1973), 2333-2346.
- [10] S. Ryu, T. Takayanagi, “Holographic derivation of entanglement entropy from AdS/CFT,” *Phys. Rev. Lett.* **96** (2006) 181602
- [11] V.E. Hubeny, M. Rangamani, T. Takayanagi, “A covariant holographic entanglement entropy proposal,” *JHEP* **0707** (2007) 062.
- [12] P. Calabrese, J.L. Cardy, “Entanglement entropy and quantum field theory,” *J. Stat. Mech* **0406** (2004) P06002.
- [13] M. Bañados, C. Teitelboim, J. Zanelli, “The black hole in three dimensional spacetime,” *Phys. Rev. Lett.* **69** (1992) 1849-1851.

- [14] M. Bañados, A. Gomberoff, C. Martínez, “Anti-de Sitter space and black holes,” *Class. Quant. Grav.* **15** (1998) 3575-3598.
- [15] R. D’Inverno, *Introducing Einstein’s Relativity*. Oxford, New York: Oxford University Press, 1992.
- [16] T. Hartman, “Lectures on Quantum Gravity and Black Holes,” Cornell University, 2015.
- [17] M. Van Raamsdonk, “Lectures on Gravity and Entanglement,” University of British Columbia, 2016.
- [18] S. Carroll, *Spacetime and Geometry: An Introduction to General Relativity*. Harlow, Essex: Pearson Education Limited, 2014.
- [19] D.C. Kay, *Tensor Calculus*. United States: McGraw-Hill Education, 2011.
- [20] E.ourgoulhon, “Conformal Killing Operator,” in *3+1 Formalism in General Relativity: Bases of Numerical Relativity*. Berlin Heidelberg: Springer-Verlag, 2012.
- [21] J. Ponce de Leon, “Embeddings for general relativity,” *Class. Quantum Grav.* **32** (2015) 195018.
- [22] C.A. Ballón Bayona, N.R.F. Braga, “Anti-de Sitter boundary in Poincarè coordinates,” *Gen. Rel. Grav.* **39** (2007) 1367-1379.
- [23] Y. Wu, “A Very Introductory AdS/CFT,” University of Chicago, 2016.
- [24] O. Madden, S.F. Ross, “Quotients of anti-de Sitter space,” *Phys.Rev. D* **70** (2004) 026002.
- [25] D. Brill, “Black Holes and Wormholes in 2+1 Dimensions,” arXiv:gr-qc/9904083 (1999).
- [26] M.Bañados, *et. al*, “Geometry of the 2+1 Black Hole,” arXiv:gr-qc/9302012 (1993).
- [27] C. Kittel, H. Kroemer, *Thermal Physics*. New York, New York: W.H. Freeman and Company, 1980.
- [28] M. Le Bellac, *Quantum Physics*. New York, New York: Cambridge University Press, 2006.
- [29] J. Cardy, “Operator content of two-dimensional conformal invariant theory,” *Nucl. Phys. B* **270** (1986) 186.

- [30] S. Ryu, T. Takayanagi, “Aspects of holographic entanglement entropy,” arXiv:hep-th/0605073 (2006).
- [31] M. Parikh, P. Samantray, “Rindler-AdS/CFT,” arXiv:1211.7370 [hep-th] (2012).
- [32] S. W. Hawking, “Black hole explosions?” *Nature* **248** (1974).
- [33] S. A. Fulling, “Nonuniqueness of canonical field quantization in Riemannian space-time,” *Phys. Rev. D* **7** (10) (1973), 2850-2862.
- [34] M. D. Kruskal, “Maximal extension of Schwarzschild metric,” *Phys. Rev.* **119** (5) (1960), 1743.
- [35] D. V. Schroeder, *An Introduction to Thermal Physics*. United States: Addison Wesley Longman, 2000.
- [36] M. E. Peskin, D. V. Schroeder, *An Introduction to Quantum Field Theory*. Canada: Perseus Books Publishing, 1995.
- [37] T. Lancaster, S. J. Blundell, *Quantum Field Theory for the Gifted Amateur*. New York, New York: Oxford University Press, 2014.
- [38] J. Louko, D. Marolf, “Single-exterior black holes and the AdS-CFT conjecture,” *Phys. Rev. D* **59** (1999) 066002
- [39] J. Louko, “Single-exterior black holes,” *Lect. Notes Phys.* **541** (2000) 188-202.
- [40] A. B. Zamolodchikov, “Irreversibility of the flux of the renormalization group in a 2d field theory,” *JETP Lett.* **43** (1986) 730-732.
- [41] J. R. Taylor, *Classical Mechanics*. United States: University Science Books, 2005.
- [42] J.D. Brown, M. Henneaux, “Central charges in the cononical realization of asymptotic symmetries: An example from three-dimensional gravity,” *Commun. Math. Phys.* **104** (1986) 207-226.
- [43] E. Verlinde, “On the holographic principle in a radiation dominated universe,” arXiv:hep-th/0008140 (2000).
- [44] G. C. Wick, “Properties of Bethe-Salpeter Wave Functions,” *Phys. Rev.* **96** (4) (1954), 1124-1134.
- [45] G. W. Gibbons, S. W. Hawking, “Action integrals and partition functions in quantum gravity,” *Phys. Rev. D* **15** (10) (1977), 2752.

- [46] S. Carlip, C. Teitelboim, “Aspects of black hole quantum mechanics and thermodynamics in (2+1)-dimensions,” *Phys. Rev D* **51** (1995) 622-631.